20513-6006-R0-00

STUDY OF A
COMET RENDEZVOUS MISSION

FINAL TECHNICAL REPORT
VOLUME II - APPENDICES

MAY 12, 1972

"This work was performed for the Jet Propulsion Laboratory, California Institute of Technology sponsored by the National Aeronautics and Space Administration under Contract NAS7-100."

(JPL Study Contract No. 953247)

TRW SYSTEMS GROUP
One Space Park
Redondo Beach, California

APPENDICES CONTAINED IN VOLUME II

APPENDIX A

RELATIVE POSITIONS OF COMET, EARTH AND SUN

1. BIPOLAR COORDINATES

A "bipolar" plot of the comet's trajectory with respect to earth and sun is a useful device in the graphical analysis of viewing conditions and other related tasks. Figure A-1 explains the projection method by which

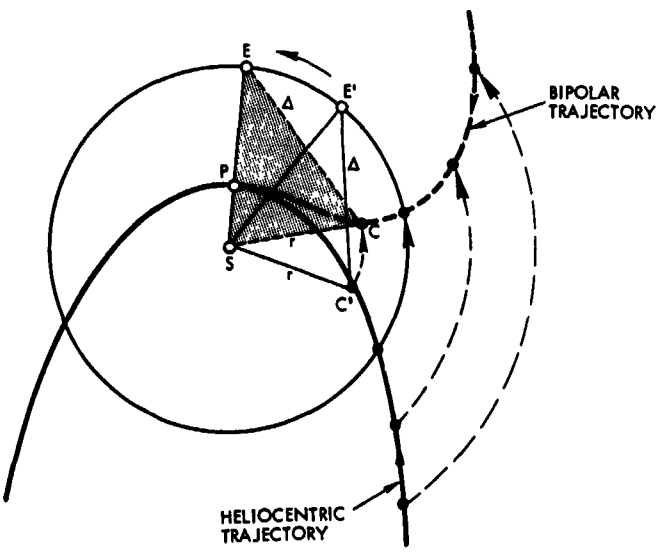

Figure A-1. Construction of Bipolar Comet Trajectory

this relative trajectory is obtained from the comet's heliocentric trajectory. For convenience of explanation we have taken the earth's reference position exactly opposite the comet's perihelion, although this is not a requirement, and we consider only the projection into the ecliptic plane. Out-of-plane coordinates can be taken into account without difficulty if desired.

Figure A-2 shows the resulting bipolar trajectory plot of Encke, in the ecliptic plane, for an extended time period on both sides of the perihelion passage, with time markers shown along the plot. This bipolar trajectory is the same regardless of the year of apparition, except that for the different years earth is moved to the heliocentric positions that correspond to the dates of the comet's perihelion passage.

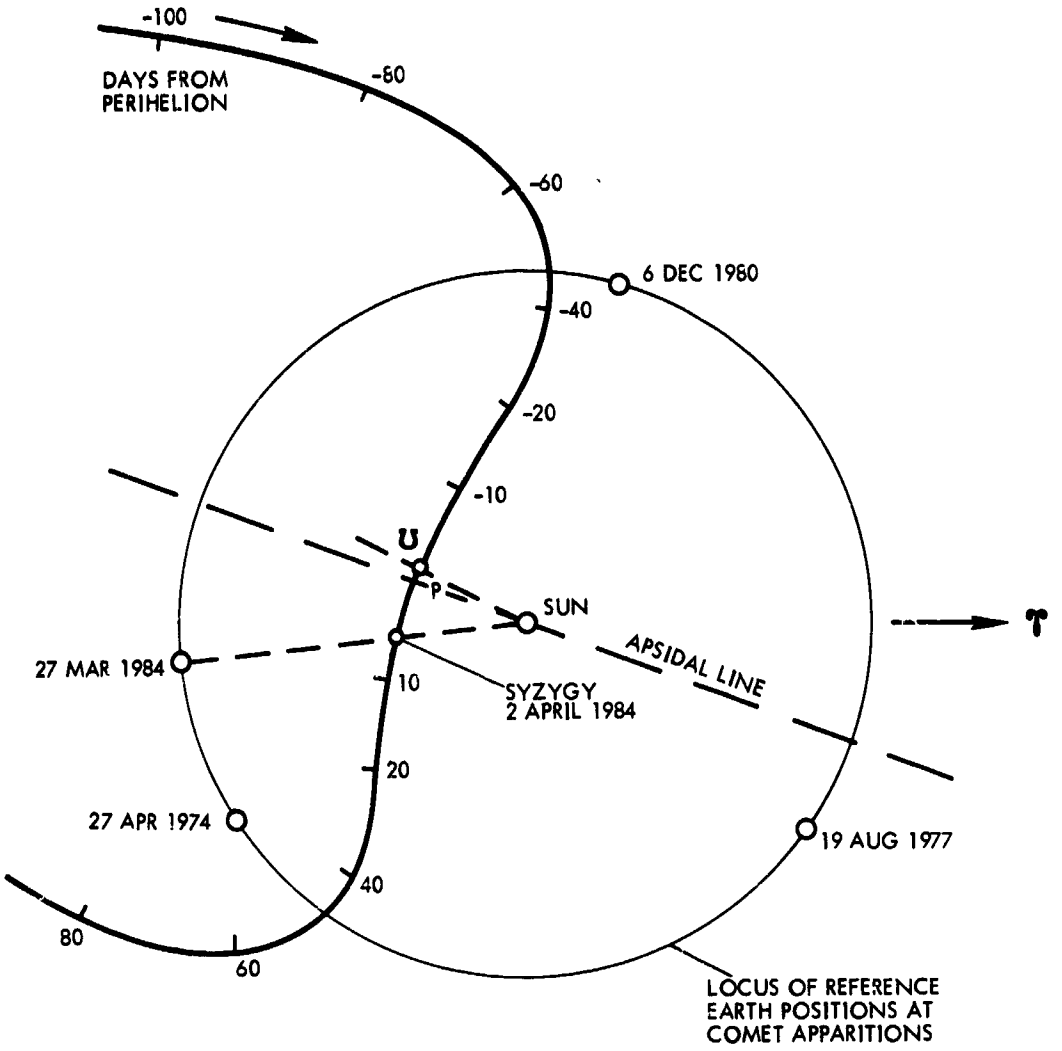

Figure A-2. Encke Relative Trajectory Projected into Ecliptic Plane (Bipolar Coordinates)

Thus the 1 AU circle in this graph becomes the locus of discrete earth reference positions as illustrated for the 1974, 1977, 1980 and 1984 passages of Encke. These positions are separated by 111.5 degrees in accordance with the 3.31-year period of Encke's orbit. Similar relative positions occur every third apparition.

2. GRAPHICAL ANALYSIS APPLICATIONS

This graphical presentation has many useful applications in comet mission analysis. It can be used, for example, to show the change in viewing geometry from earth to comet and vice versa. In Appendix B it is used to illustrate and explain the differences in the observability of

Encke in many of its past apparitions. The plot also permits direct graphical determination of communication ranges, earth-probe-sun angles, and probe viewing angles from DSIF stations during the post-rendezvous phase when the probe's position coincides with the comet's. Special events can be readily identified such as communications blackout that occurs at syzygy. A plot of circles of constant range and constant view angles (see Figure A-3) can be used as a transparent overlay to facilitate graphical analysis of the relative viewing geometry from earth or spacecraft.

With regard to the coming apparitions of Encke in 1974, 1977, 1980 and 1984 the following characteristics in viewing conditions from earth can be directly ascertained by inspection of Figure A-2.

1) During the 1977 apparition the comet will be acquired late, and viewing during the perihelion passage is poor.

2) 1980 is favorable for early acquisition. A spacecraft arriving 40 to 50 days before perihelion has a minimum communication range at that time. Communications blackout cannot occur in this mission year.

3) 1984 is favorable for early recovery and provides good communication conditions throughout the rendezvous and stationkeeping phase. However, there will be a communication blackout for several days as the comet and spacecraft pass in front of the sun.

4) Conditions for comet tail observation from earth are best in earth positions such as 1980 and 1984. Positions such as 1977 practically rule out tail observation. This illustrates in part the conclusion on tail observability stated before.

5) The 1974 apparition offers a unique opportunity for extended observation of Encke after the perihelion passage because of the strategic relative position of earth: e.g., during the 60-day period between $P + 15^d$ and $P + 75^d$ the earth-comet distance is less than 0.5 AU. With viewing conditions quite similar to those during the anticipated 1984 rendezvous mission, the 1974 apparation is of particular interest from a program preparation standpoint with respect to comet recovery timing, loss of observability from earth, etc.

Figure A-4 illustrates specific relative geometry aspects of the 1984 mission opportunity. In addition to time marks, the plot shows the variation of the earth-probe (comet)-sun angle, and ranges centered on earth.

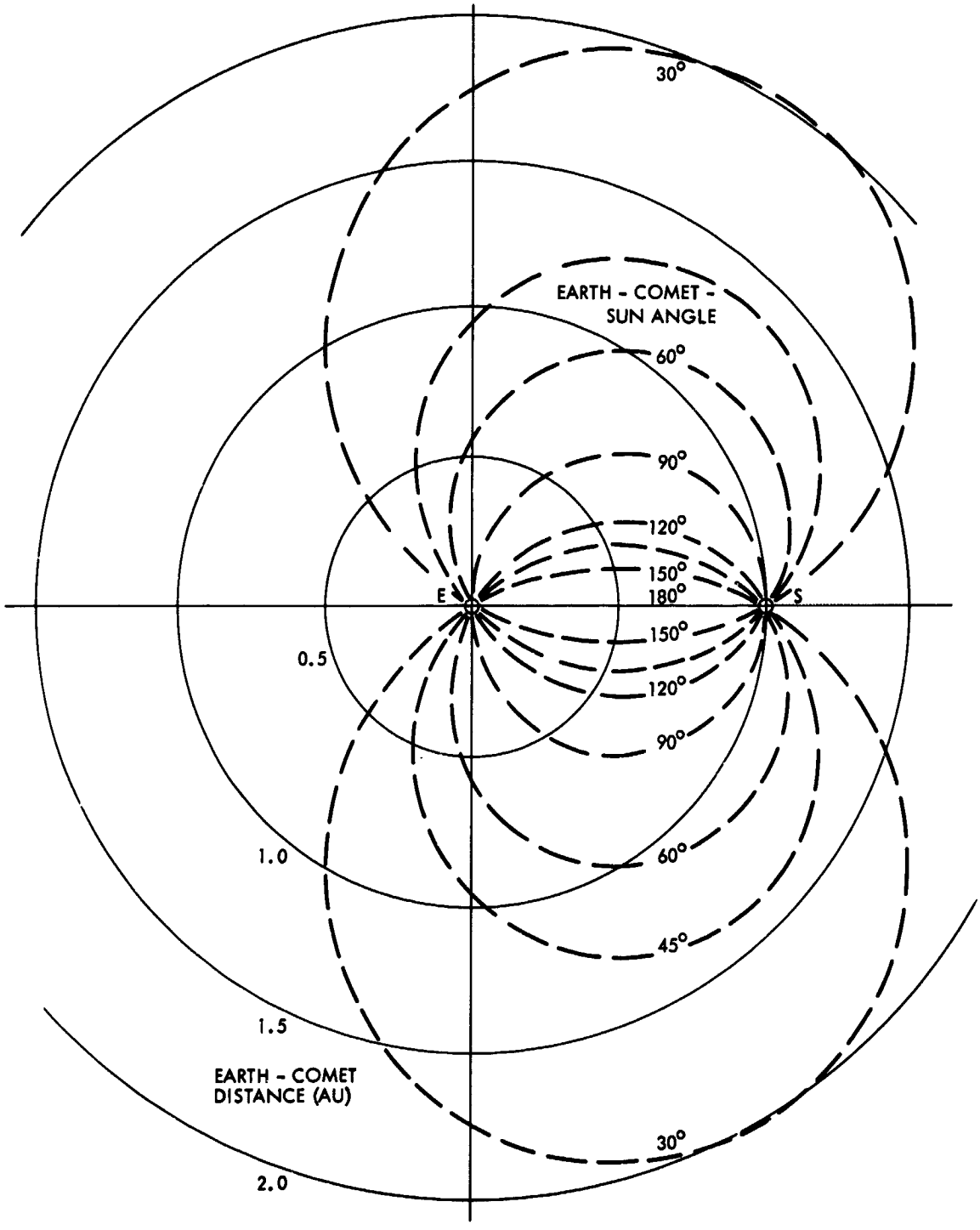

Figure A-3. Circles of Constant Distance and View Angle

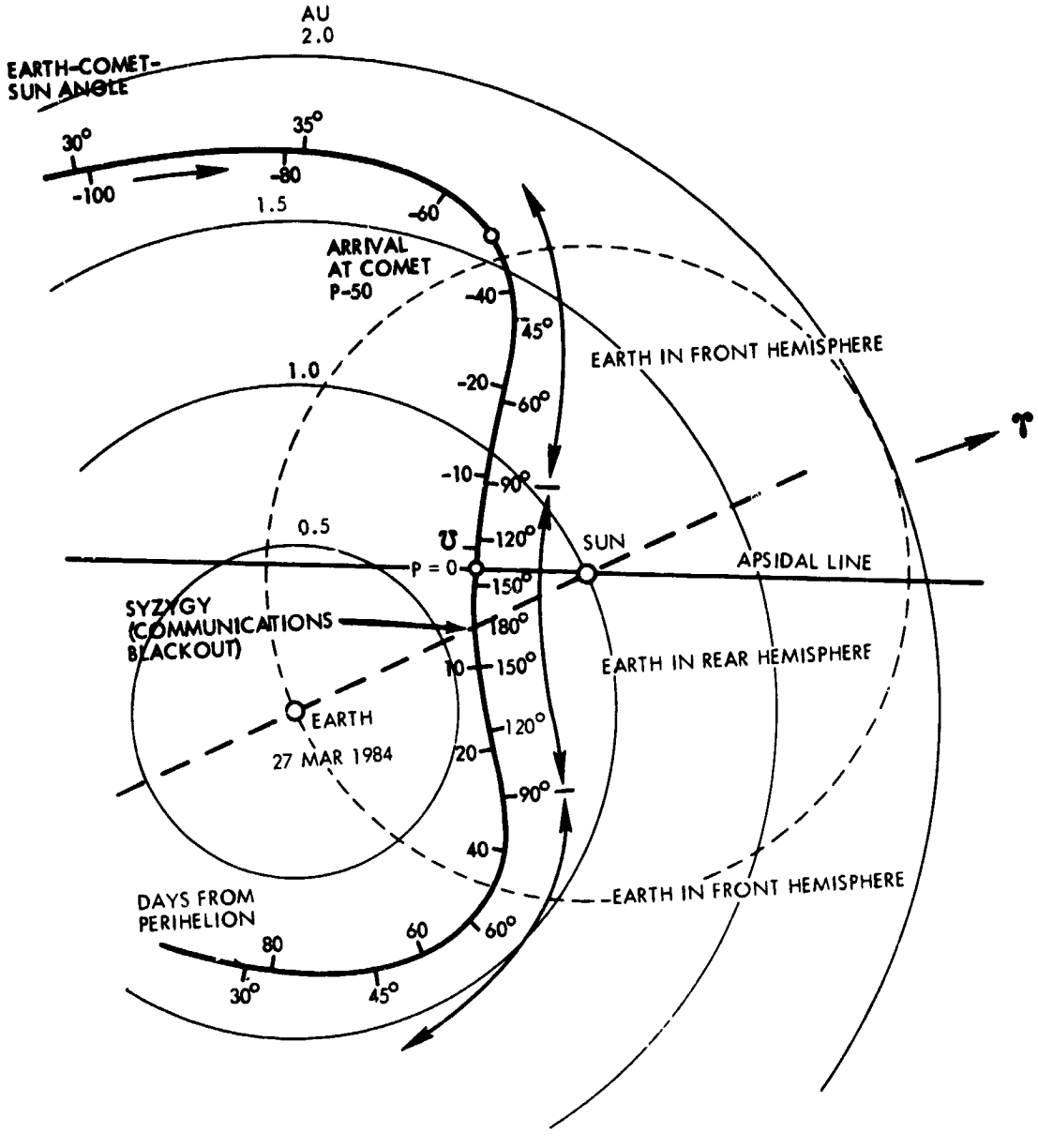

Figure A-4. Earth-Comet-Sun Positions for 1984 Mission

During the time interval from P - 9 days to P + 30 days the earth is in the rear hemisphere as seen from the sun-oriented spacecraft. At these times the position of the high-gain antenna must be reversed. Conjunction occurs not long after the descending node passage. At conjunction the comet and spacecraft reach about 7°S heliocentric latitude. As seen from earth they appear in a position of about 3.5 degrees below the ecliptic plane. Therefore the possibility of a one- to two-day communications blackout caused by solar radio noise must be anticipated.

3. DETERMINATION OF APPARENT COMET MAGNITUDE

Since the bipolar plot directly displays the relative distances from earth (Δ) and sun (r) as functions of comet position and time from perihelion it permits convenient determination of apparent magnitudes as observed from earth. Using the equation

$$\Delta m = m - m_o = 2.5 \log \Delta^2 r^{2n}$$

with n = 2

contours of constant magnitude increments Δm can be obtained in terms of the coordinates of the bipolar plot. Figure A-5 shows these magnitude contours for Δm values from +7 to -4. This graph can be used as a transparent overlay with the extended bipolar plot of the same scale (Figure A-6) to determine the apparent magnitude variation of the comet

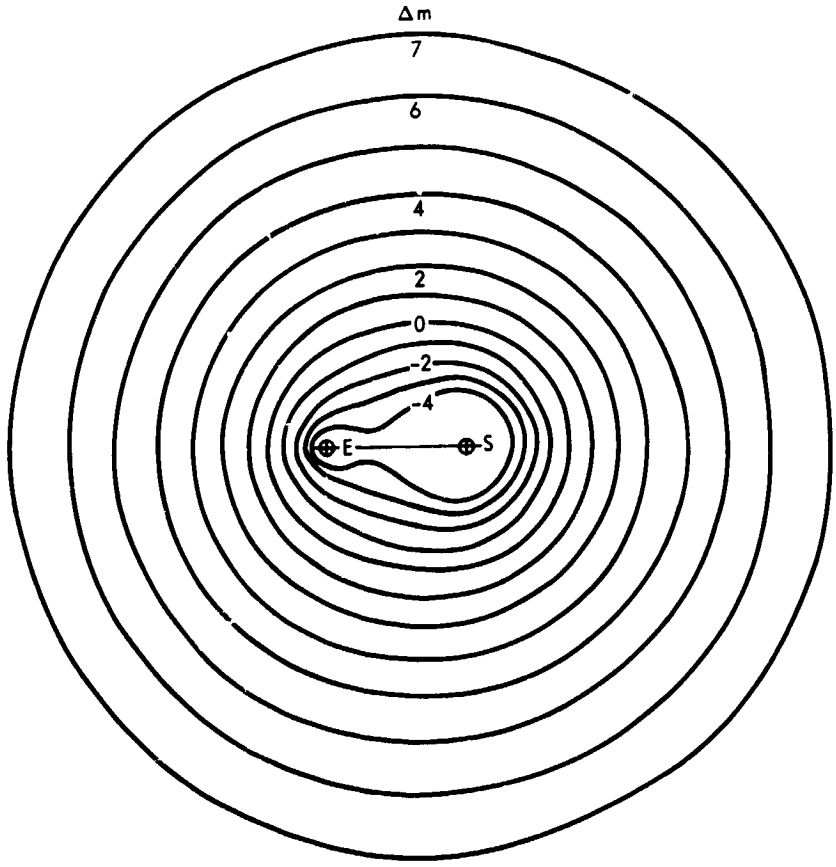

Figure A-5. Contours of Constant Magnitude

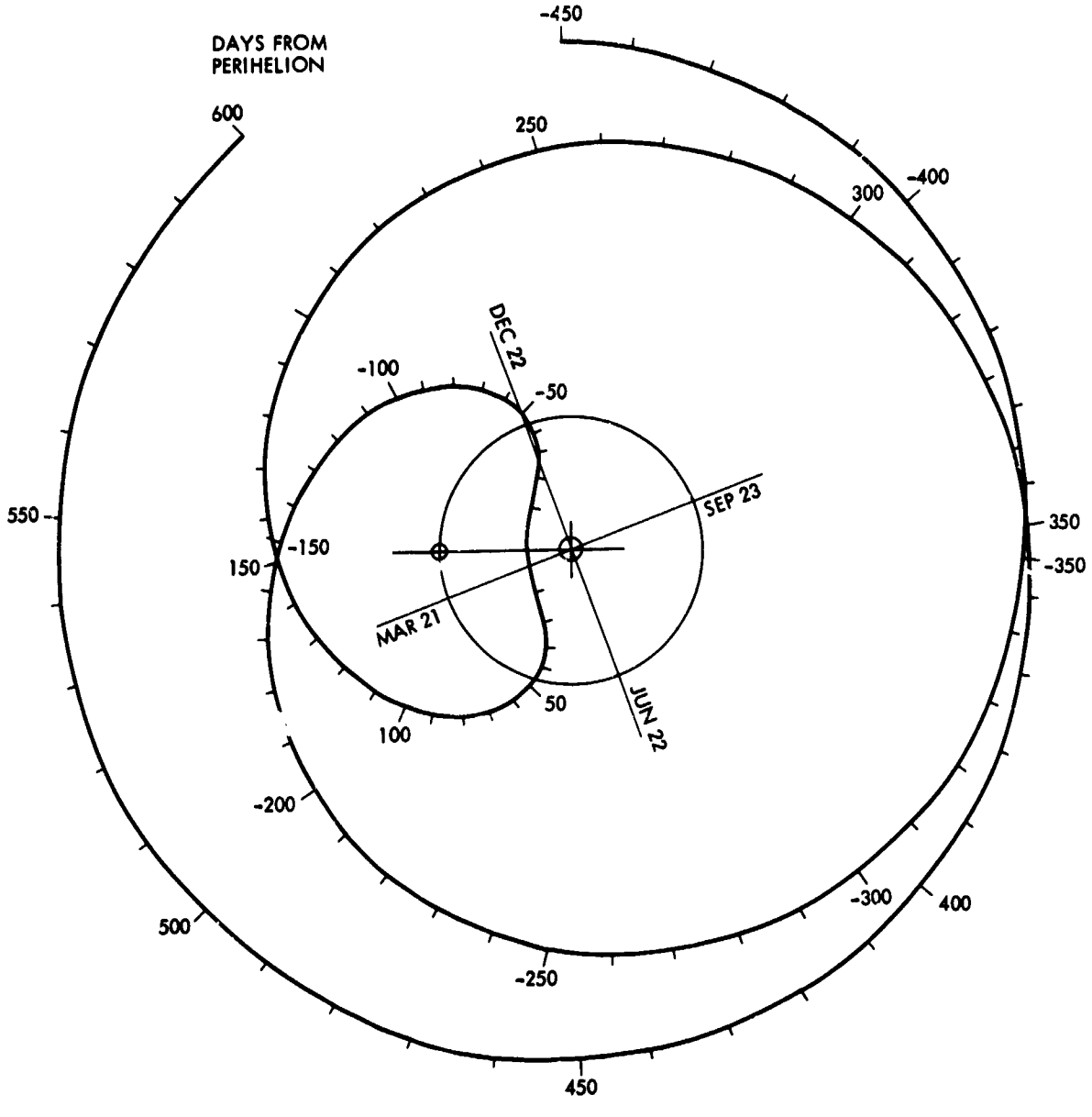

Figure A-6. Extended Bipolar Plot of Encke

along the trajectory for any year of apparition. The earth-sun baseline of Figure A-5 must be lined up with the specific earth location of the year in question.

This technique was used to obtain a contour of magnitude 17.5 (using $\Delta m = 5$ and the comet reference magnitude $m_o = 12.5$) which is shown in Figure A-7 superimposed on the extended bipolar plot, for conditions averaging the 1974 and 1984 apparitions. This gives a conservative estimate of the time of comet recovery. (Actually, under favorable conditions, the comet can be recovered at magnitude 18 to 19).

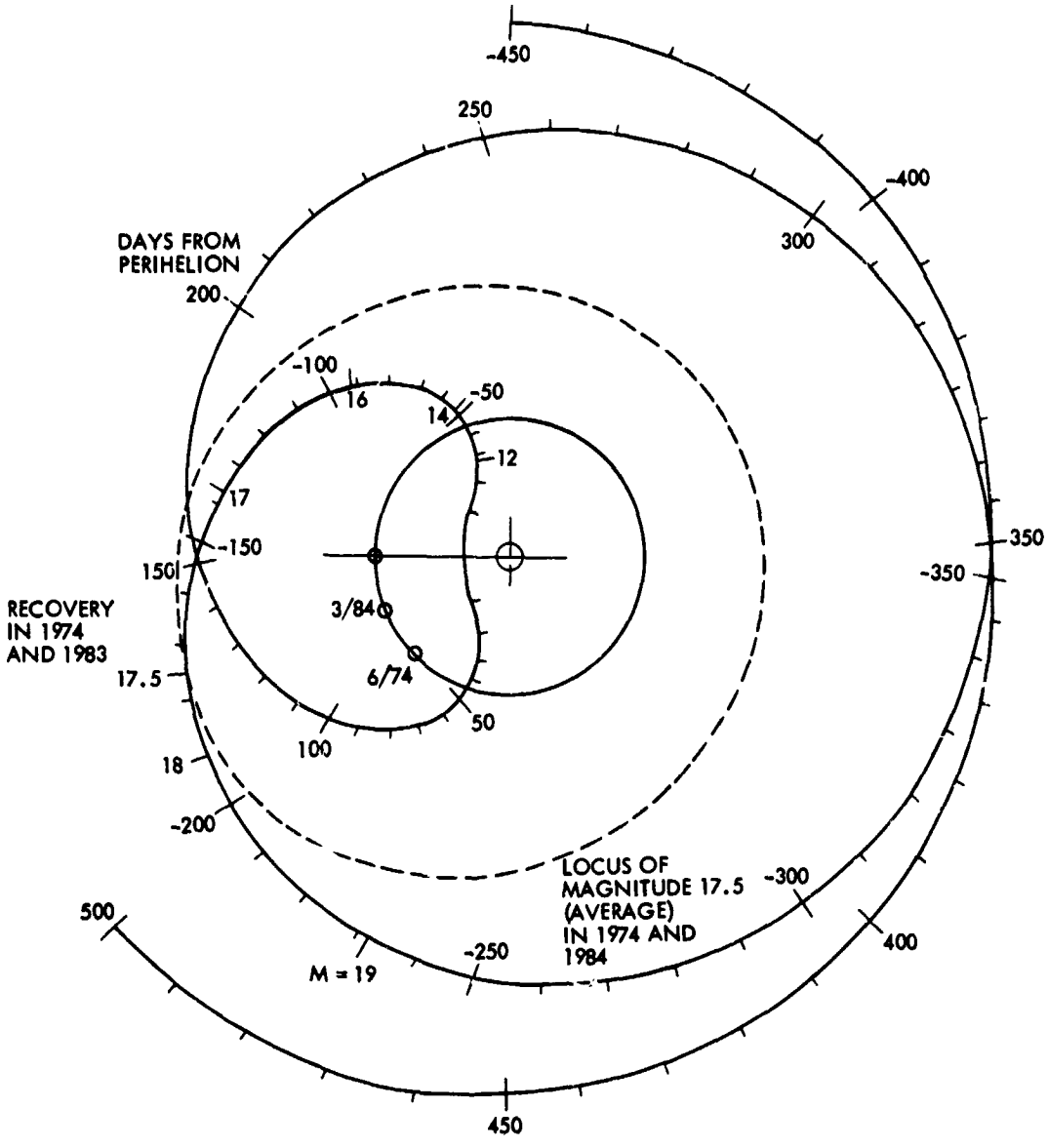

Figure A-7. Comet Magnitude Variations for 1974 and 1984 Apparitions

This occurs about 175 days before perihelion. Other m-values are marked along the inbound trajectory, e.g., m = 17 at P - 137^d, m = 16 at P - 92^d, m = 14 at P - 48^d, etc. We note that 1974 and 1984 are years favoring early recovery since the earth relative locations are opposite incoming comet positions at 180 and 200 days before perihelion, respectively. If earth were in opposite location (least favorable for early recovery) the comet would reach magnitude 17.5 much later, about 115 days before perihelion.

APPENDIX B

A GRAPHIC HISTORY OF VIEWING CONDITIONS FOR P/ENCKE

The capability of earth-based telescopes to recover Encke on a given pass has depended heavily, though not exclusively, on the moving geometric arrangement of earth, sun, and comet during that pass. Not all configurations are equally favorable to recovery or sustained observation. Since Encke's perihelion is inside the earth's, the comet's periodic location in the daylight and its alignment with the sun constitute one important factor adversely affecting its visibility. The diminished brightness of Encke and its southern locus after perihelion are additional factors. An ideal rendezvous mission would occur when observations of Encke from earth are likely to be extensive.

The 3.3-year period of Encke determines that particular sun-earth-comet relationships should be repeated approximately every ten years. Reproduction of the pattern every decade is not perfect, however, so that passes separated even by 20-year intervals present sets of viewing angles significantly different from each other. Comparison of earlier viewing conditions is facilitated by use of the bipolar form of Encke's orbit described in Appendix A. Figure B-1 displays the bipolar version of Encke's orbit, together with the earth's perigee position, for all 20 apparitions from 1885 to 1951, inclusive. The solid segments of the orbital traces represent the portion or portions of the comet's orbit over which it was observable, not necessarily continuously observed, on each pass (taken from Vsekhsvyatskii's data, Appendix J).

The patterns of observability divide themselves naturally into three groups, designated in the figure by letters A, B, and C. In the apparitions of Group A, the comet was recovered both before and after perihelion; in those of Group B, recovery occurred only after perihelion; in those of Group C, only before perihelion. Two apparitions are unlettered, since they seem to belong decisively to none of the three categories, i.e., when the perigee locations of the earth are examined (see below). The brief observation in 1941 may be attributable in part to wartime conditions. Indeed, there was no recovery at all in 1944. The perigee location of

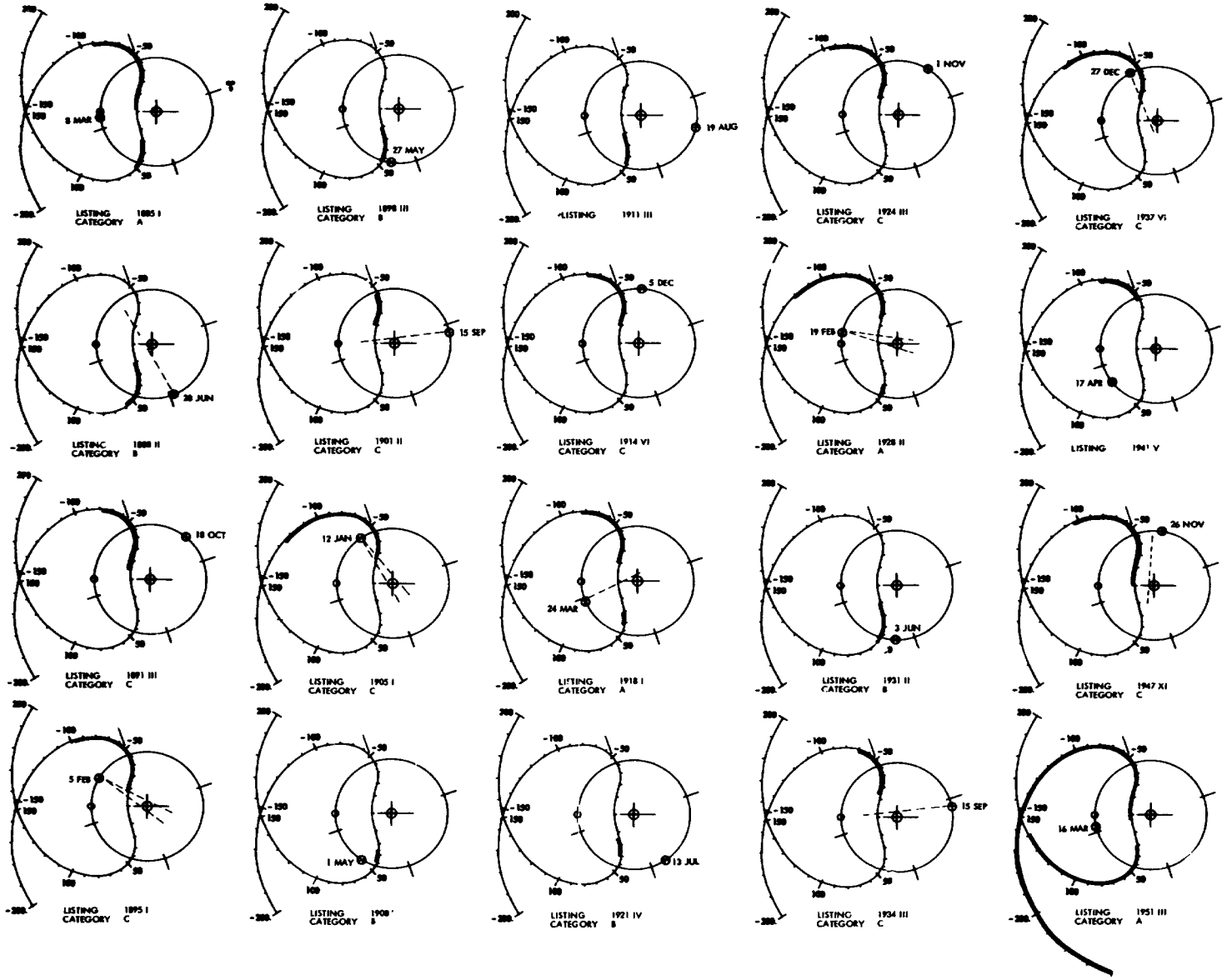

Figure B-1. History of Encke Observations 1885 to 1951 (Bipolar Coordinates)

of earth for the 1941 apparition should have put it in Group A, especially since 1941 was a year of moderate solar activity and the comet's visibility would be expected to have been better than average.

In general, whenever acquired inbound, Encke is recovered by the time it reaches 1 AU, some 50 days or so before perihelion, which is about the time the planned 1984 rendezvous would begin. The patterns of Figure B-1, however, point to Group A as providing the best viewing situations experienced in observing the comet. The geometry associated with this group has permitted, as a rule, the most favorable combinations of early recovery, long observation, visibility close to perihelion, and rerecovery after perihelion of all analogous cases. Perihelion times of this group were all between 19 February and 24 March. Perihelia of Encke in late winter or early spring therefore define those passes most favorable to long-term coordinated earth-based and on-site measurements, and the 1984 perihelion of 27 March corresponds to just such a pass.

The history of viewing conditions reviewed here covers a century of observation by equipment and with techniques which might be regarded today as obsolete. Although it is recognized that the best available modern facilities would be devoted to Encke during a rendezvous mission, it must be assumed that significant dependence on visual observation, especially by amateurs, will play a role in such a mission, particularly for monitoring of temporal variations. The historic record of viewing conditions is therefore quite relevant.

APPENDIX C

DETECTION OF ENCOUNTERS WITH TAURID METEOR STREAMS

This Appendix presents an analysis of the rate of expected meteoroid encounters, attributable to Taurid meteor streams, during the transfer of the spacecraft to its rendezvous with comet Encke. Since the Taurids are assumed to have originated from Encke there is considerable interest in obtaining flux and composition data of these meteoroids, particularly of those streams that are not crossing the earth orbit and have thus remained unobserved. This analysis refers to the cruise phase mission objectives discussed in Section 6 of Volume I.

1. DISCUSSION

There are several effects which make it very difficult to predict the probability of a spacecraft encountering a given meteoroid stream and recognizing, through meteoroid detectors, that the encounter has occurred. A variety of numbers enter into the calculations and most of these numbers are uncertain. Some of the principal questions involved are listed here, and consequences of different assumptions are discussed.

Considering the Taurid meteor streams in particular, a short list of questions reads like:

1) What is the total mass in the Taurid streams? This requires assumptions as to the original mass and present age of comet Encke and the percentage of emitted mass that is particulate matter as compared to gaseous matter.

2) How many Taurid streams are there and what is the mass in each stream? Since several (at least seven) separate streams are identified as striking the earth there may well be more (100?). In this case the total mass ejected by the comet will be distributed in some fashion among them. The line of apsides of the comet appears to have moved with time, giving rise to the many streams. A major question is why this should occur. If the movement is gradual, a small angular displacement of the line of apsides with each revolution, one would expect the

cometary debris to be smeared out over a large volume of space, rather than as discrete streams. If the movement of the line of apsides is in jumps, say because of perturbations received in the asteroid belt after several revolutions, the debris could be left in more or less distinct streams, but how many is impossible to say.

3) What is the diameter of a meteor stream? The earth moves along its orbit about 2.5×10^6 km/day so a four-day meteor shower would indicate a chord length (or minimum diameter) of 10^7 km. The Taurids actually last for several weeks but they are classified as several showers of a few days duration each.

A subsidiary problem is the distribution of the matter in the stream along the orbit. Due to various perturbations the ultimate distribution will probably be uniform around the orbit, but this process is throught to take hundreds of years. Streams that are much younger than this might more properly be called swarms since most of the material will be distributed along a short length (1/10 ?) of the orbit. In this case, merely crossing the orbit will not guarantee detection of a significant number of meteoroids.

Another possible complication concerns the observation that in some streams there appears to be a "fine structure." The total stream diameter may be 10^7 or more km, but within the stream particles are bunched into filaments of much smaller diameters. The activity of the Giacobinids (Reference 1) is strongly suggestive of this type of structure. Because the activity of the Taurid streams is low, any such fine structure would not appear to earth-based observations but could be significant to a spacecraft attempting to detect the stream.

4) What is the size distribution of the mass in the stream? The number distribution of interplanetary particles is presumed to vary systematically with mass, smaller particles always predominating. Whipple's famous curve (Reference 2) has the cumulative number of particles varying as mass to the (-1.34) power. A better curve which considers more data is the NASA meteoroid environmental model (NASA 1969). It follows the Whipple curve down to a particle mass of about 5×10^{-6} gm and then has the cumulative number varying as mass to

the (-0.5) power. This curve predicts considerably fewer small particles than would the extension of the Whipple curve. It is this NASA curve which we assume predicts accurately the background against which the meteor stream must be detected.

The particulate matter emitted by a comet is almost bound to have a different size distribution but it is unknown. Millman (Reference 3) analyzes the earth-based data on seven meteor showers (Leonids, Quadrantids, Geminids, Perseids, Aquarids, Lyrids, Orionids) and concludes the N versus m slope is less steep than the -1.34 used by Whipple. Whipple's curve comes from nonshower or "background" meteors. The absolute number of particles in the showers is such that they produce more large meteors (say about 10^{-2} gm) than background but because of the lower slope produce less small meteors (below about 10^{-4} gm) than background. He concludes "...the strong annual meteor showers seem to have little effect on the background particle flux for masses less than 10^{-6} gm."

While these observations do not apply directly to the Taurid streams, other observations indicate the Taurids are probably similar. Wetherill states that the absence of continuum radiation from the coma of Encke indicates that not more than about 10 percent of the ejected particulate matter can be in the form of small (a few millimeters or less) particles. Several authors (Whipple, Hawkins) observe that the Taurid showers appear to have more than a normal percentage of bright meteors (about 1 gm) and fireballs (several kilograms and up).

5) How has the distribution of particles in the stream changed due to various perturbing effects – Poynting-Robertson, radiation pressure, orbit perturbations from asteroids and Jupiter? The Poynting-Robertson effect causes a tangential retarding force on any particle in orbit and in time will cause the particle to spiral into the sun. The time required is proportional to the particle radius and density. On the other hand, the radiation pressure force is directly opposite to the gravitational force and the ratio of radiation force to gravitational force varies inversely as the particle radius and density and is independent of the distance from the sun. When this ratio, β, is greater than one, the particle will move out of the solar system. When β is less than unity, the particle sees a

smaller effective gravitational force. The critical value of β is less than unity for a particle originally in an elliptical orbit, as the orbit will be changed to hyperbolic. The exact value depends on the eccentricity of the original orbit (see Figure C-1).

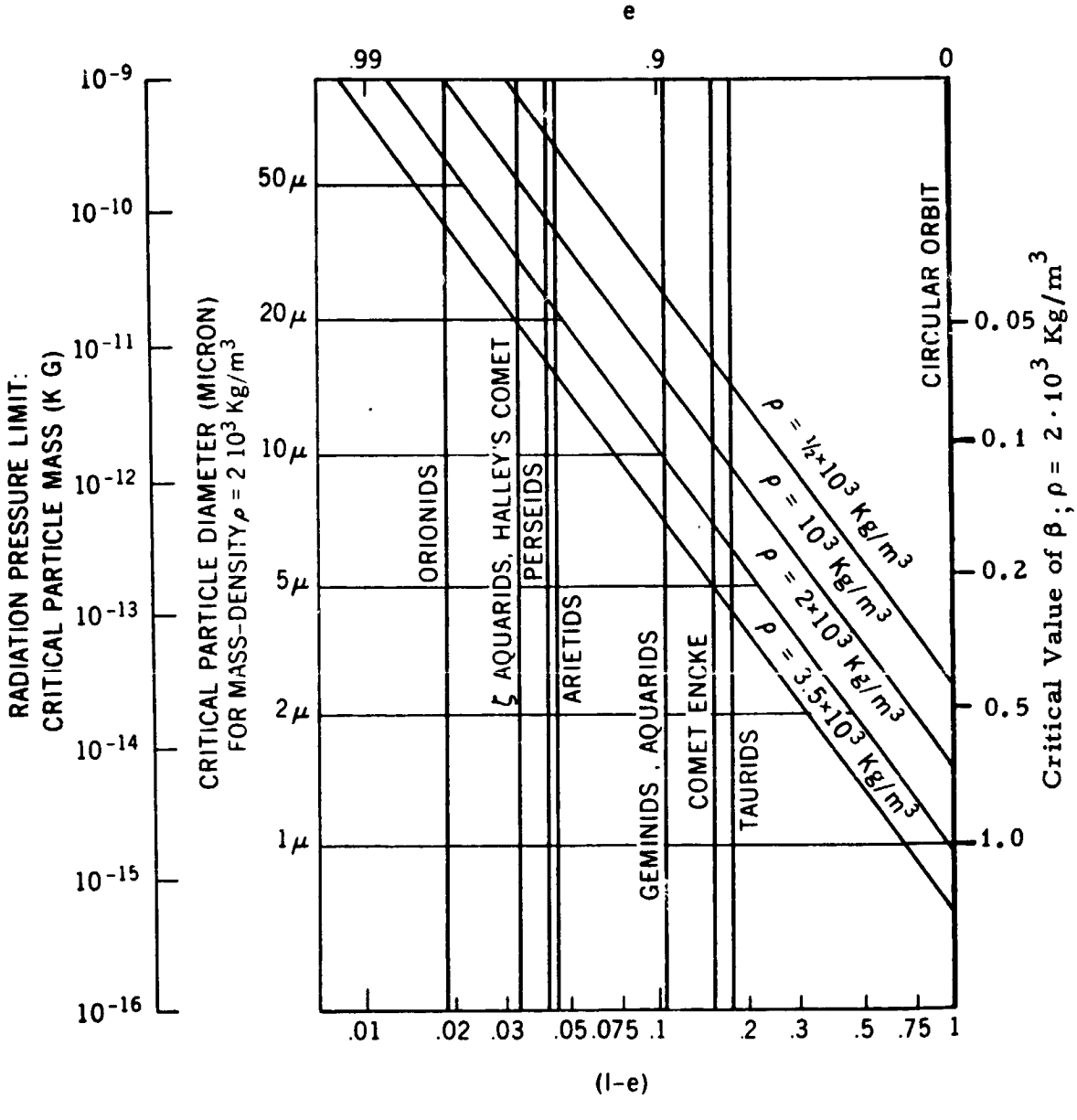

Figure C-1. Radiation Pressure Limit for Several Streams and Comets as a function of Particle Densities and Eccentricities

Figure C-2 is a plot of the Poynting-Robertson effect as a function of particle mass with some radiation pressure limits indicated. The

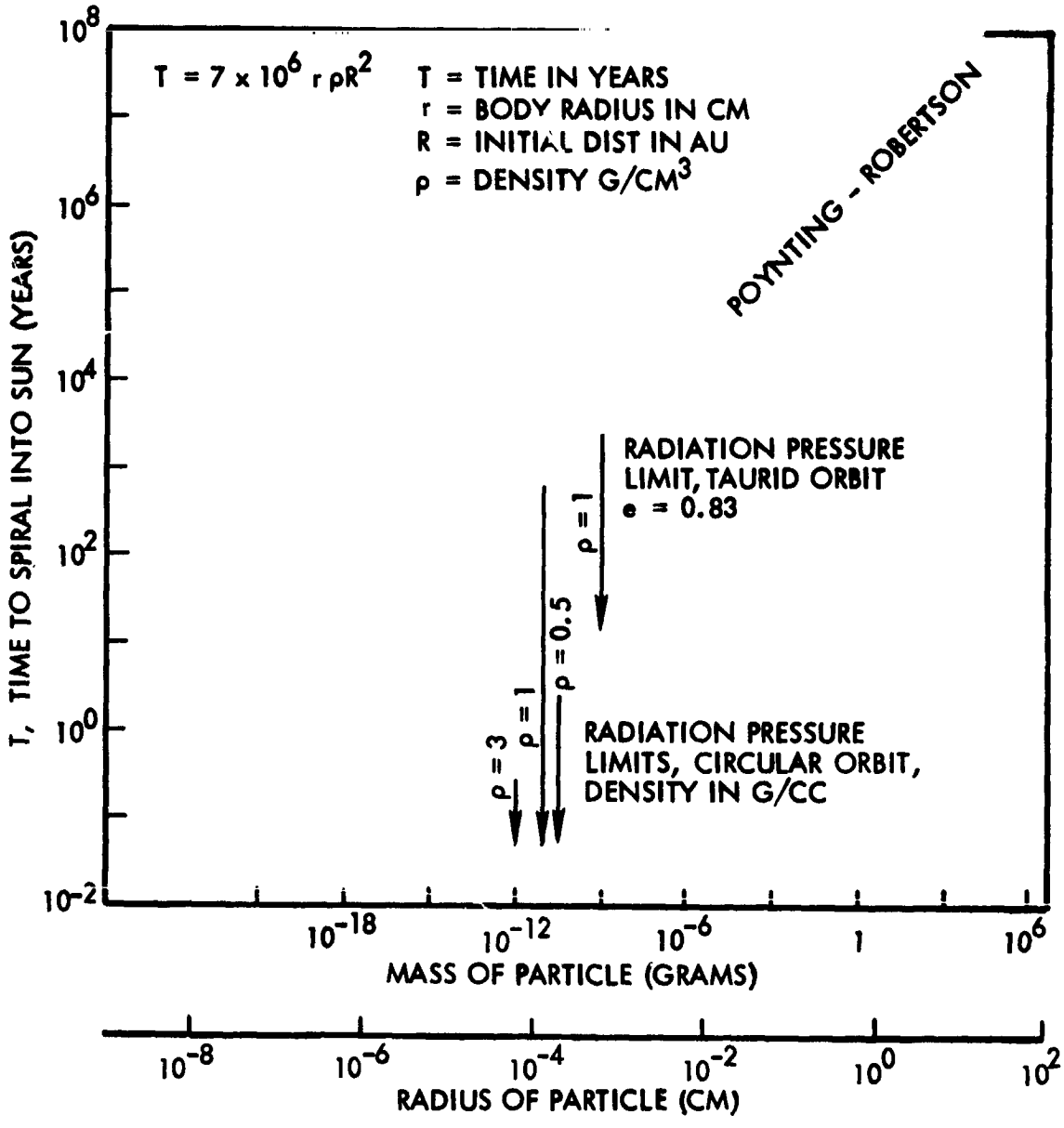

Note: In Figures C-1 and C-2 the critical values of the ratio β = solar pressure/solar gravity force are related to the critical particle diameter r_c by

$$\beta_c = 5.8 \cdot 10^{-5}/\rho\ r_c$$

Figure C-2. Poynting-Robertson Effect at 1 AU and Particle Density 1 g/cm³

radiation pressure limit is 10^{-9} gm for particles* originally in an orbit of eccentricity about 0.83. At this mass the Poynting-Robertson time is about 5000 years. While the age of Encke is not known, 5000 years is an upper limit. On this basis then the Poynting-Robertson effect should not influence (very much) particles from comet Encke. Those with a mass somewhat less than 10^{-9} gm will move into a hyperbolic orbit and cannot be older than about a year. Those with a mass somewhat greater than 10^{-9} gm will have Poynting-Robertson times around 10,000 years or more and should not have spiraled very far towards the sun, with the possible exception of the very oldest particles.

Other perturbations will by this time have dispersed the material in the older streams more or less uniformly around the orbit. The time scale for this process is probably a couple of hundred years. There also appears to have been a westerly movement of the line of apsides of comet Encke, so that if the meteor streams are crossed from the east, the older ones will be encountered first. Provided useful information can be obtained in the stream crossings, it will be neatly separated as to age.

2. CALCULATIONS

The assumptions necessary to calculate the expected encounter rate in a Taurid stream are listed below.

1. The total emitted mass of particulate matter is 5×10^{15} gm, midway between Wetherill's estimates of 10^{16} and 2×10^{15} gm. This may be conservative.

2. We consider two cases, one large stream, of about 4×10^{7} km diameter and ten smaller streams, of about 4×10^{6} km diameter. The length of the streams is equal to the orbit of Encke. These numbers define the volume within which the total ejected particulate matter is spread. Note that as far as number density is concerned, one large stream of 4×10^{7} km diameter is exactly equivalent to 100 smaller streams, each with one percent of the total matter, and diameter 4×10^{6} km. Other assumptions about stream diameter and/or number will affect the results in an obvious way.

*Assuming $\rho = 1$ as the particle density

3. Two size distributions of particles are assumed. In both the cumulative number N varies as

$$N = k/m^{\alpha}$$

where k is a constant related to the total mass, m is the mass of a particle and α is the slope of the cumulative number-mass line. Calculations are made for two values of α, $\alpha = 1$ and $\alpha = 0.7$. The case $\alpha = 1$ is a long-standing assumption while $\alpha = 0.7$ is closer to the observations of Millman on meteor streams. The constant k is calculated from the relationship

$$\text{Total mass} = 5 \times 10^{15} \text{ gm} = \int_A^B m \, dN$$

The lower limit of mass is taken as 10^{-8} gm, since the radiation pressure limit for Taurids appears to be about 10^{-7} gm. The upper limit of mass is taken as 10^3 gm. In the case of $\alpha = 1$ this upper limit is unimportant, by the nature of the curve. Varying the upper limit from 1 gm to 10^6 gm changes the cumulative number at any mass by less than a factor of two. In the case of $\alpha = 0.7$ the upper limit is more important. Integrating to 10^6 gm instead of 10^3 gm lowers the number of particles at a given mass by about a factor of 10. Consequently, an upper limit of 10^3 is used in both cases.

$$k(\alpha = 1) = 2.0 \times 10^{14} \qquad k(\alpha = 0.7) = 2.7 \times 10^{14}$$

The circumference of Encke is 11.1 AU = 1.67×10^9 km. The total volume in the case of one stream of 4×10^7 km diameter is 2.1×10^{33} m^3. The number of 10^{-8} gm particles is

$$(\alpha = 1) \qquad 2.0 \times 10^{14}/10^{-8} = 2 \times 10^{22}$$

$$(\alpha = 0.7) \qquad 2.7 \times 10^{14}/10^{-5.6} = 1 \times 10^{20}$$

The number density of particles in the two cases is

$$(\alpha = 1) \quad n = 20 \times 10^{22}/2.1 \times 10^{33} = 9.5 \times 10^{-12} \ (m^{-3})$$

$$(\alpha = 0.7) \quad n = 1 \times 10^{20}/2.1 \times 10^{33} = 4.8 \times 10^{-14} \ (m^{-3})$$

The impact rate f per m^2 is the number density times the relative velocity, assumed to be 30 km/sec. Thus

$$(\alpha = 1) \quad f = 2.85 \times 10^{-7} \log N = -6.54 \text{ (impacts/m}^2\text{-sec)}$$

$$(\alpha = 0.7) f = 1.44 \times 10^{-9} \log N = -8.84 \text{ (impacts/m}^2\text{-sec)}$$

The case of the same amount of material in ten streams each of 4×10^6 km diameter will yield an impact rate in any given stream which is 10 times higher than the numbers above. Therefore, these curves are plotted in Figure C-3 as bands one order of magnitude thick.

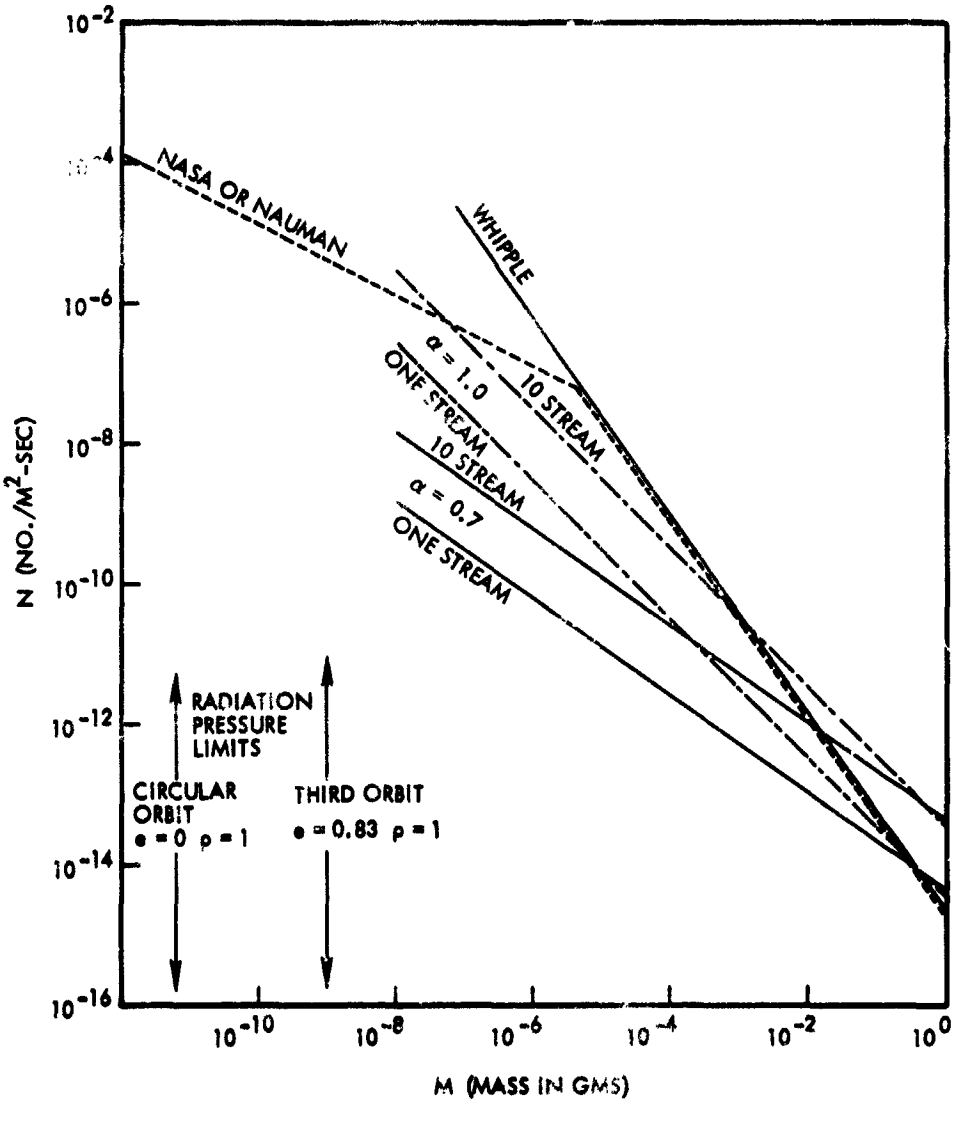

Figure C-3. Particle Size Distribution in Meteoroid Streams

3. CONCLUSIONS

As might be expected the curves show an expected encounter rate in excess of background for particles in the 0.1 gm and up region. It is particles in this size range that cause visible and radio meteors when they strike the earth's atmosphere. Occurring only during the transit of the stream, they cause the meteor shower. However, the probability of a spacecraft detecting a particle of this size is extremely low. The Sisyphus meteorite detector, which detects particles by their reflected sunlight and therefore scans a larger volume of space than conventional impact detectors is suitable for large particle detection.

Figure C-4 is a plot of the expected Sisyphus count rate on a Venus-Mercury mission. The expected particle flux that has been used to draw this curve is the same flux that is labeled NASA in Figure C-3, i.e., it corresponds to our background rate. If the meteor stream has a flux a factor of ten higher than background at a given mass than the resulting Sisyphus count would be a factor of 10 higher at that mass than shown in Figure C-4. Cheerfully extrapolating the Sisyphus curve yields an expected rate of about 2×10^{-3} events per day per decade mass at 10^{-1} gm and about 3×10^{-4} at 1 gm. Thus, even if the meteor stream flux at these masses is a factor of 10 above background the expected events per day are very low.

The smaller particles in Figure C-3, around 10^{-8} or 10^{-7} gm, are those which can be detected and composition-analyzed in detectors of the impact ionization type. Composition measurements are potentially of great interest. Unfortunately it appears that the expected flux is about equal to or well below background. This conclusion cannot be helped much by assuming a different mass distribution. For example if the total mass of 5×10^{15} gm is assumed to be in the form of 10^{-8} gm particles (an unrealistic assumption) the encounter rate at 10^{-8} gm only rises a factor of 25. Assuming a larger total mass of course will raise the curves proportionately as will assumptions which distribute the mass throughout a smaller volume.

One other point should be brought out. It relates to the experience of Mariner IV. Alexander (Reference 4) reports the microphone sensor

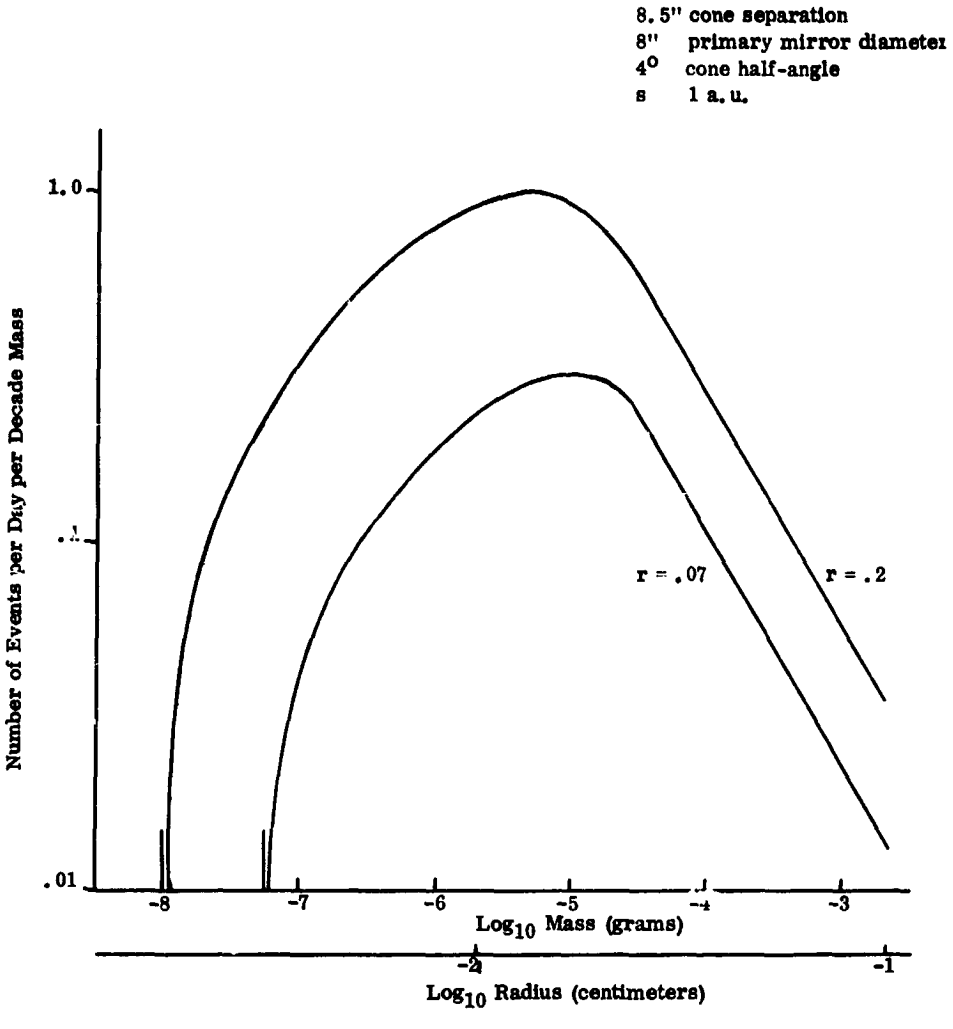

Figure C-4. Differential Curve for Mariner Venus/Mercury 1973 Event Rate Based on Assumed Penetration Flux

on Mariner IV detected a sharply increased counting rate (17 impacts in 16 minutes compared to a background rate of about one per day) when the spacecraft was located at R = 1.27 AU, celestial longitude +343.6°, latitude +2.25°. Microphone impact detectors are known to give erroneous indications at times and a certain amount of caution is advised in accepting this result. On the other hand, the sensor had performed predictably for more than two years before the event and continued to do so for several months afterwards.

Alexander ascribes this event to particles from comet Encke, spiraling into the sun, but this appears unlikely. A more reasonable explanation would seem to be an encounter with a Taurid meteor stream.

If the spacecraft, more or less cutting across the orbit, was moving at 20 km/sec, then it travelled 1.9×10^4 km during the 16 minutes of the event. This could indicate that material in the stream, while dispersed around the orbit, is in relatively small filaments within the stream. The significance of this is that even with a background rate of one or several per day, a short time period burst of impacts is easily separated from background and identified as a separate event.

REFERENCES

1. Gerald S. Hawkins, "Meteors, Comets and Meteorites," McGraw-Hill, New York, 1964.

2. F. L. Whipple, J. Geophys. Res., 68, 4929 (1963).

3. Peter Millman, "Meteor Showers and Interplanetary Dust," Cospar, Space Research X, Prague, May 1969.

4. W. M. Alexander, C. W. Arthur, J. D. Corbin and J. L. Bohn, "Mariner IV and OGO III," Twelfth Cospar Meeting, Prague, 1969.

APPENDIX D

EPHEMERIS OF COMET ENCKE

Nongravitation perturbations of comet Encke have been determined to a high degree of accuracy from past observations (see Section 2) such that changes in the ephemeris from one apparition to the next can be predicted with great confidence. Dr. B. G. Marsden reports* that predictions of the January 1971 passage required the remarkably small correction of only $+5 \times 10^{-4} \pm 10^{-4}$ days based on observations during October to December 1970 although "this close agreement may be somewhat fortuitous." The small ephemeris changes expected to occur in the 1974, 1977 and 1980 apparitions of Encke are as follows, according to Marsden:

Orbit Elements		1974	1977	1980
T	(date)	1974 Apr. 28.9988 E.T.	1977 Aug. 17.0087 E.T.	1980 Dec. 6.5787 E.T.
ω	(deg)	185.9277	185.9521	185.9784
Ω	(deg)	334.2246	334.2118	334.2000
i	(deg)	11.9823	11.9391	11.9463
q	(AU)	0.338116	0.340654	0.339933
e		0.847456	0.846477	0.846762
a	(AU)	2.216521	2.218905	2.218339
p	(yr)	3.30	3.31	3.31
Epoch	(date)	1974 Apr. 23.0 E.T.	1977 Aug. 5.0 E.T.	1980 Nov. 17.0 E.T.

In computing the spacecraft transfer trajectories presented in Section 5 we used the 1980 ephemeris as predicted in the above table. Actually a still more refined 1984 Encke ephemeris could be obtained from this by taking the 1980 elements and running them with a n-body program to 1984 and applying afterwards a small correction (-0.02 ± 0.04 days). However, this degree of refinement was not necessary for purposes of this preliminary mission study.

*Personal communication, 11 November 1971.

Section 5.5.3 quotes typical ephemeris uncertainties also based on Marsden's data, which reflect in the relatively small navigational errors that will be corrected by onboard observations as discussed before.

APPENDIX E

APPLICATION OF SOME MICROWAVE AND OPTICAL TECHNIQUES USEFUL IN A COMET RENDEZVOUS MISSION

This appendix presents a brief description of a radar altimeter for use in the comet rendezvous mission. Its primary purpose is to support gravity measurements by providing the exact distance from the spacecraft to the nucleus. Some potential alternative uses for the altimeter both in its simplest form and with augmented capabilities are also suggested. The use of an optical driftmeter as backup instrument for velocity and angular rate measurements is discussed. In addition, a rough estimate is made of the feasibility of radar sounding of both the nucleus and coma of the comets Encke and D'Arrest from earth.

1. RADAR ALTIMETER

1.1 INTRODUCTION

Altimeters using propagation time measurements have been routinely used in aircraft for a long time. There are two basic types and several hybrids. The following paragraphs briefly describe these varieties.

1.1.1 The FM-CW Altimeter

This type employs a continuous wave transmitter, and relies on integrating the Doppler frequency shift of the energy reflected from the approaching or receding surface. An initial value of altitude is required. System noise and reference oscillator stability determine the smallest detectable frequency shift. The magnitude of the returned signal, which in part depends on the transmitter power and the operating frequency determines

the time to obtain a measurement. Since a CW oscillator is used prime power limitations and oscillator efficiency limit the transmitted power. This variety of altimeter finds its greatest utility at ranges up to a few thousand feet.

1.1.2 Pulsed Altimeter

The use of a rather large ratio of peak to average power makes this variety of altimeter equivalent to a range-only radar. The altitude is sampled at the pulse repetition frequency of the transmitter. Isolation between transmitter and receiver determines the lowest altitude at which a pulsed altimeter may be used. The greatest altitude depends on the transmitted power and the reflectivity of the surface.

1.1.3 Hybrids

The basic altimeter function is range determination. On that basis there are many modulation structures which can provide range. One variety of hybrid approach is the use of a sinusoidal transmitted signal which is phase modulated by $\pm \pi$ at intervals corresponding to a known pseudo-random noise (PRN) code. The range determination consists of correlating the waveform returned after scattering from the surface with a stored replica and determing the value of time delay required to obtain a correlation peak. This time is the two-way range. Such PRN modulations allow all the transmitter power to be used, and to obtain good range resolution because PRN waveforms exhibit sharp correlation peaks.

The accuracy of all radar altimeters is affected if the reflection process smears out the time dependence of the transmitted waveform. If the transmitted beamwidth is too broad a system employing Doppler frequency shift will lose accuracy because of the variation of line-of-sight velocity within the beamwidth.

1.2 APPLICATION TO COMET RENDEZVOUS

A basic altimeter for use in the range of 10 Km to 100 Km would have to be of the pulsed variety or employ PRN modulation. To contain the comet (diameter = 4 Km) at the longest range (100 Km) a transmit/receive antenna about 0.75 meter in diameter would be needed at 10 GHz.

An estimate of the signal power required for altimetry is useful in both "sizing" a basic altimeter and also for evaluation of the utility of a more complex radar altimeter which might obtain other information about the comet.

The ratio of received to transmitted power for equal transmitting and receiving apertures A, at target range R and transmitted wavelength λ is:

$$\frac{P_R}{P_T} = \frac{A^2}{(\lambda R)^4}\,\sigma A_t$$

where A_t is the interception area of the target and σ is the scattering cross section. The target diameter is less than a beamwidth.

The radar cross section of a target depends upon its size relative to the radar wavelength, details of its surface structure and on its material. A perfectly conducting (a metal) sphere large compared to the wavelength intercepts an amount of radiation corresponding to its projected geometrical area and reradiates this energy. Radar cross sections are sometimes reported as an equivalent area of a sphere. If the sphere (radius r) is of a dielectric material, then the cross section σ is:

$$\sigma \approx \rho\,\pi\,r^2$$

where ρ is the reflection coefficient corresponding to normal incidence given by:

$$\rho = \frac{(1 - \sqrt{\epsilon})^2}{(1 + \sqrt{\epsilon})^2}$$

where ϵ is the dielectric constant of the target sphere. If the surface of the sphere is irregular then in some directions the reflections will add in phase, and in other directions out of phase producing relative maxima and minima in the cross section. Cross sections are usually averaged over a range of angles, and where there is relative motion between target and receiver, are also averaged over a time long compared with the fading period. The fading period is the time during which the cross section goes from a maximum to a minimum in the case of relative motion. For irregular spheres the cross section is usually written:

$$\sigma = g \rho \pi r^2$$

where the factor g (the gain) contains the dependence of the cross section on the surface irregularity. Some special cases have been worked out.

For an undulating surface where the rms slope is α

$$g \approx 1 + \alpha^2$$

If the surface is rough with a scale length equal to the wavelength

$$g > 1$$

The observations on irregular objects give the product

$$g \rho$$

For long wavelengths $g \rightarrow 1.0$ and then the corresponding values of measured cross section can be taken as estimates of the dielectric constant.

The power ratio can then be written:

$$\frac{P_R}{P_T} = \frac{A^2}{(\lambda R)^4} \; g \rho \pi r^2 A_t$$

For the case where the beamwidth is entirely filled by the target surface

$$A_t = \pi \left(\frac{\lambda}{D}\right)^2 R^2$$

where D is the diameter of the altimeter antenna.* Therefore:

$$\frac{P_R}{P_T} = \frac{A^2}{(\lambda R)^4} g \rho \pi^2 r^2 \frac{\lambda^2 R^2}{A}$$

and

$$\frac{P_R}{P_T} = \left(\frac{\pi}{\lambda R}\right)^2 g\rho A r^2$$

For a comet nucleus the quantity $g\rho$ might be quite small if frozen gases were the primary constituents. The presence of solid rocky crystalline matter would however increase this reflectivity. For an estimate $g\rho = 5 \times 10^{-2}$ will be used. For the moon $g\rho \approx 7 \times 10^{-2}$ because of the broken and porous nature of the surface.

For $R = 10^5$ meters
$\lambda = 0.03$ meters
$A = 0.56$ meter^2
$g\rho = 5 \times 10^{-2}$
$r = 2 \times 10^3$ meters

$$\frac{P_R}{P_T} = 4 \times 10^{-5}$$

The receiver noise power P_n level is:

$$P_n = N k T \Delta f$$

* This area is about the same as that of the first Fresnel zone whose diameter is $\sim \pi R\lambda$

where N = receiver noise figure

k = Boltzmann's constant (1.38×10^{-23} joule/°K)

T = Receiver temperature

Δf = Receiver noise bandwidth

For N = 10

T = 290°K

$\Delta f = 10^8$ Hz

$$P_n = 4 \times 10^{-12} \text{ watt}$$

System implementation losses including pointing and polarization might amount to a signal loss of an additional factor of 10 resulting in a transmitter radiated power of 10^{-3} watt with a S/N = 30 dB. The bandwidth corresponds to a pulse width of about 10 ns, and a range resolution of 3 meters. Because the rendezvous craft is moving with respect to the comet a substantial portion of this S/N would be taken up by the deep fading to be expected with an irregular target surface. These transmitter and receiver requirements are extremely modest and could be implemented with present technology using all solid state components. Reference 1 describes a balloon borne altimeter using one watt peak power at a wavelength of 70 cm which was used from 2 to 20 km from the earth. A possible mechanization of the altimeter might involve the

---

Reference 1: Levanen, N and Stremler, F.G., "Accurate Pulse Radar Altimeter for Meteorological Balloons", Proc. IEEE 57 1680 (1969).

use of the 1.8 meter diameter S-band telemetry antenna as the altimeter antenna. This option could provide for a back-up altimeter for the 0.75 meter antenna system used in the preceding estimate and provide for the possiblity that the spacecraft would be limited to stand off at a distance of 100 km from the comet.

1.3 POTENTIAL USES OF A MICROWAVE ALTIMETER

There are some cometary constituents and effects which might be re-remotely probed by means of a microwave sensor, i.e., a more complex version of the radio altimeter discussed here. The general nature of the effects is that their detection and analysis could provide cometary diagnostic information from microwave backscatter, self emission or absorption. The table below summarizes these possibilities.

COMA EFFECT OR CONSTITUENT	COMMENT
Free Electron Plasma	Electron density is very low. Use of a very high power transmitter and a very sensitive receiver might allow detection of incoherent scatter from free electrons. (Thomson scatter) The echo might be difficult to discern from the solar wind electron echo.
Charged Free Radicals (OH^*)	Similar problem as with free electrons except in addition the "best" frequency for back scatter would be substantially lower due to greater mass of the radical.

Plasma Turbulence at Contact Discontinuity	Dimensional scale or magnitude of gradients unknown.
Particles of Bulk Matter	Presumably found in coma from disruption of rocky inclusions in nucleus.

In Sections 5 and 6 (Volume I) extended station keeping in the penumbra of the nucleus was considered as a method of providing thermal protection near perihelion. This could be modified to a station keeping mode in the umbra proper if the spacecraft carries a rechargeable battery of sufficient capacity to last through intermittent periods of total solar eclipse. The eclipsed position offers unique advantages to do remote probing of the coma without the interference of direct sun light. Scattering, emission, and absorption phenomena can be observed from this vantage point at large as well as small angles from the direction of solar radiation. Some species in the coma might be detectable by their own emissions such as the neutral atomic hydrogen (H) (1420 MHz), the radical OH (1665 MHz) and molecular water (H_2O) (22 GHz, 183 GHz, and many lines extending to about 24 μm in the infrared). Such emission or absorption measurements in the microwave range would employ a microwave radiometer. Most of the effects detectable by backscatter would also be detectable by use of the sun as a source.

All of the radical and molecular species mentioned have absorption and emission spectra in the visible or near visible spectral range. Such observations from the umbra would be useful.and could be compared intermittently with measurements in sunlight for calibration purposes. Observations toward the sun from the edge of the umbra, against the limb of the nucleus, would reveal absorption characteristics of the most dense part of the gas envelope.

For the case of the particulate species in the coma, measurements (probably optical) of the scattered solar radiation in orthogonal polarizations would be particularly useful. Such measurements would give evidence of particle size, shape and alignment. However, a microwave radar could also be used to detect such particles, although its operating frequency would best be in the frequency region above 30 GHz ($\lambda < 1$ cm).

It is possible that a radar altimeter operating at such a frequency could also be used for remote probing of the coma. For the altimeter function the higher frequency would allow use of a smaller antenna, and at the power levels required would not press millimeter wave technology.

2. EARTH BASED RADAR SOUNDING

It is tempting to suggest that radar observations on comets might be carried out from the earth. As previously noted from inspection of Encke's relative trajectory in 1974 (see Appendix A), the earth-Comet distance is less than 0.5 AU for nearly 2 months. With the following parameters

Wavelength	0.3 meters
Range	0.3 AU
Transmitter antenna	24 meters
Receiver antenna	60 meters
Transmitter Power	500 KW
Comet Diameter	4 Km

the received power from the nucleus is about 2×10^{-25} watt. This compares with about 6×10^{-23} watt for the same radar (Goldstone) arrangement obtained

from the asteroid Icarus. Another interesting object for earth stationed radar contact is comet D'Arrest. This is a smaller comet than Encke, but its very close approach to earth in July-September 1976 (with distances below 0.2 AU for eight weeks) provides a unique opportunity for such observations.

The possibility of obtaining radar echoes from the coma should also be examined. A radar echo might be obtainable from incoherent scatter by free electrons in the coma. The receiver would probably have to range gate out such return from ionospheric electrons. The size of the visible coma suggests that it would fill the beamwidth of a radar such as the one used in the nucleus sounding. Coma electron echoes should also be discernable on the basis of the Doppler shift when the comet velocity vector is oriented along the radar line-of-sight.

3. OPTICAL DRIFTMETERS (V/H SENSOR)

The V/H sensor offers a passive optical technique for measuring the angular velocity of the platform relative to the surface over which the carrier vehicle is flying. This angular velocity is the ratio of the velocity component, V, tangential to the surface at the altitude H.

The optical V/H meter is a direct descendant of the family of devices used for measuring the drift of a platform relative to a point on a reference surface. It consists of an optical system which forms an image of the terrain on a reticle. A sketch is shown in the figure. In the simplest case the reticle is of the picket fence variety, consisting of alternately transparent and opaque elements. Usually the terrain image in the reticle surface is reimaged by a field lens onto a photodetector.

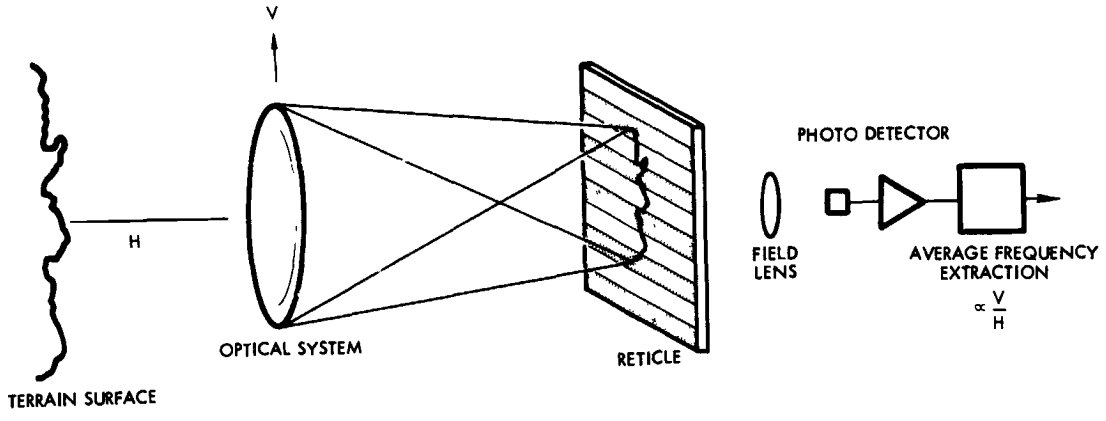

V/H Meter Functional Diagram

Operation of this device produces a wave form having a band limited frequency spectrum at the output of the photodetector.

The operation of V/H sensor depends only upon the existence of illumination gradients which can be chopped by the reticle. These gradients can be on any scale so long as they can be imaged on the reticle. For example at large distances from the surface suitable gradients might be the shadows of large surface irregularities. At very short distances the illumination gradients resulting from the inhomogeneous surface or small fissures would be used.

A combination of three equally spaced V/H sensors can resolve the two velocity components parallel to the viewed surface and the component perpendicular to the surface. Just as with the radar altimeter, the V/H sensors require an initial condition.

To improve the operation of the V/H sensor sometimes the reticle is vibrated at a known frequency. This is equivalent to applying a carrier frequency to the signal and shifting the spectrum to a higher frequency where filtering is more easily performed. The output of a V/H sensor is an average frequency which is a known function of the instrumental

parameters (reticle spacing and optical magnification). This frequency can be determined in a variety of ways. A typical approach is to hard limit the photodetector output and to count zero crossings. In this fashion the precision to which the frequency can be determined depends on the precision of the local reference. A precision of a few parts in 10^7 is easy to obtain.

4. OPTICAL AND MICROWAVE POLARIMETRY

The principal difference in the information provided by a polarimeter operating in the optical spectral region and microwave remote sounding technique is the feature scales that the two approaches resolve.

The polarimeter observes radiation which is scattered from the surface. This radiation may be transmitted from the instrument or may be ambient radation, i.e., solar radiation. Measurements are made of the scattered intensity at various azimuths with respect to the scattering surface. This angular dependence is also determined for linearly polarized radiation, both parallel and perpendicular to the plane of incidence. In the microwave range, the same sort of measurements can be implemented. The penetration depth for an electromagnetic wave in a material is measured by the skin depth. This quantity gives the distance that the electric field which enters the medium penetrates for a 1/e reduction in its magnitude. Microwave wavelengths penetrate more deeply than optical wavelengths, and are scattered by gradients of a different scale than optical waves.

The amount of microwave radiation with a given polarization reflected from a surface is a function of the angle of incidence. This function differs for different polarizations. This holds for plane boundaries which

are very large compared to the microwave wavelength. A natural surface is comprised of elements in all size ranges, and with a distribution of orientation angles. As a result it is possible for the microwave energy scattered from such a surface to be polarized predominately in a given state.

The measurement of the percentage of the energy scattered by a surface which is polarized in each of two orthogonal states can be used to deduce the properties of the surface when the wavelength and observation angles are known.

APPENDIX F

APPROACH NAVIGATION/IMAGING INSTRUMENT

1. INTRODUCTION

This Appendix presents preliminary specifications of a dual-mode approach navigation/imaging instrument for an Encke comet probe. A simplified version of the high resolution Mariner Mars 1971 television system is proposed for comet acquisition and tracking beginning at about 60 days before encounter, as well as for imaging as close as 10 km from the comet nucleus.

Also included is a discussion of the star field background expected for definition of the comet position and reducing the comet trajectory uncertainties during terminal navigation.

2. INSTRUMENT FUNCTIONS

The dual-mode approach navigation/imaging instrument is based on the Mariner Mars 1971 television instrument technology (Reference F-1). Required changes to the camera for this application include:

- Eliminate wide-angle camera and associated electronics
- Change optics to 125-mm focal length, f/2.0
- Increase maximum exposure to about 33 seconds
- Add comet nucleus detection circuitry.

A block diagram of the instruments is given in Figure F-1. The lens (125-mm, f/2) is chosen to optimize the dual-mode purpose of the sensor. The focal length provides a larger field (4.4 x 5.6 degrees) than the Mariner Mars 1971 (MM '71) narrow angle camera to improve acquisition of the comet and reference star field, while yielding adequate resolution (0.1 mrad) for imaging. An f/2 relative aperture is assumed to be the largest that will provide the point source image size of MM '71.

The shutter is assumed identical to MM '71 (~6 seconds maximum exposure), with additional signal integration to 33 seconds accomplished by multiple exposure and vidicon beam blanking.

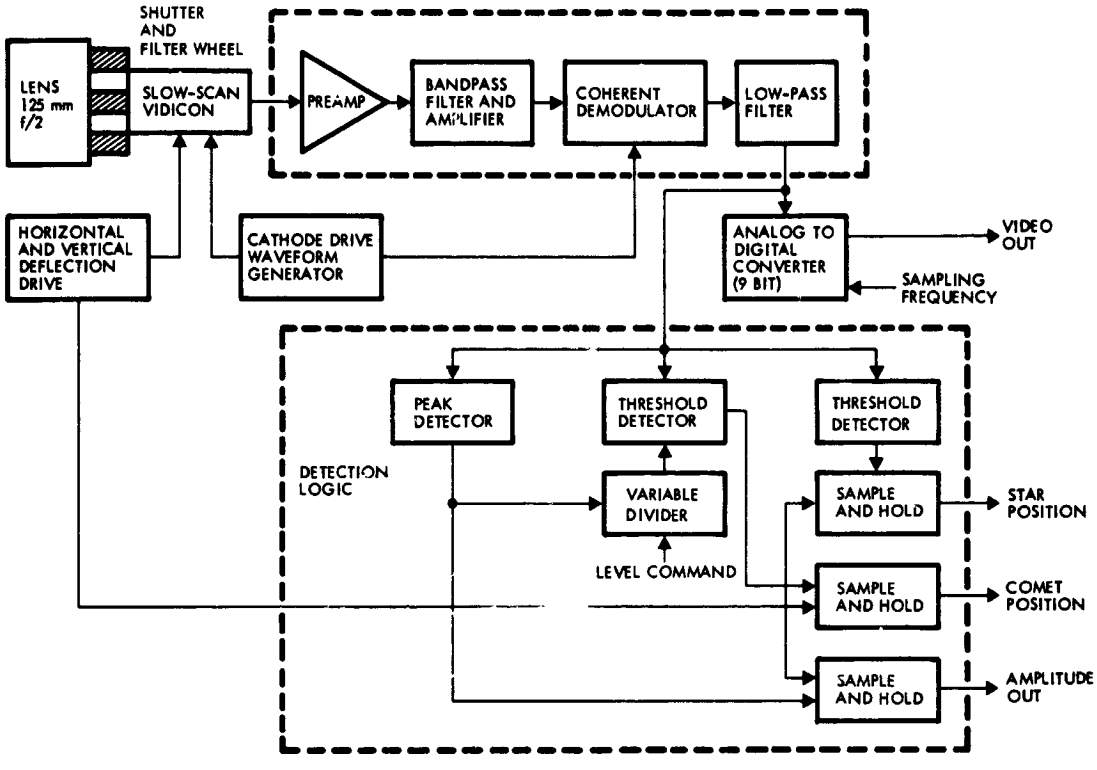

Figure F-1. Block Diagram, Approach Navigation/Imaging Instrument

A filter wheel with up to eight spectral or polarizing filters is included to provide rough photometric data regarding the comet.

A slow scan vidicon identical to MM '71 is assumed. The cathode drive modulates the scanned out vidicon target image, which is amplified, filtered, demodulated and post-filtered to provide the video signal. An A/D converter quantizes the video for data transmission.

In addition, the video signal is examined and processed by the detection logic for comet/star presence. To improve comet nucleus detection accuracy, a peak detection scheme is suggested.

Thresholding the video signal in the coma region would introduce large uncertainties inthe location of the comet nucleus (actually, the center of brightness). Assuming the comet brightness to vary as in Figure F-2, the optimum threshold level is at, or near, the peak. However, thresholding too near the peak reduces the probability of detection, considering noise.

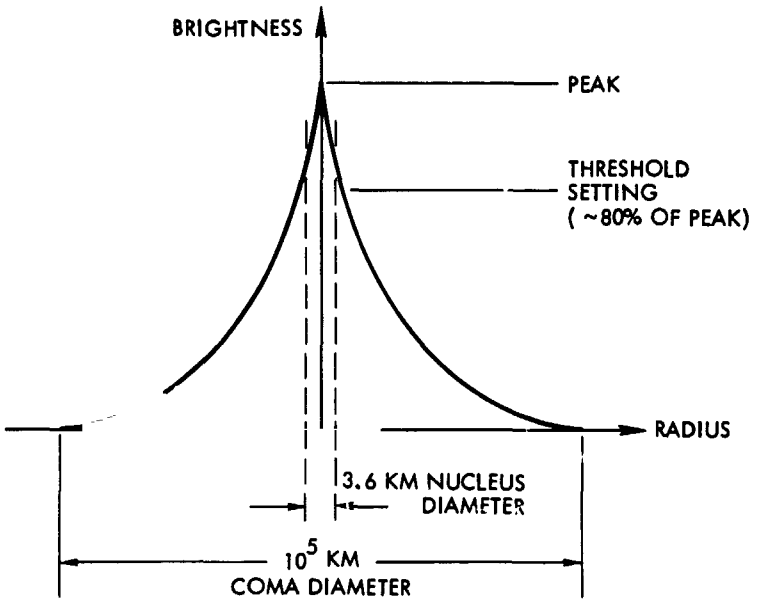

Figure F-2. Schematic Spatial Variation of Comet Brightness

Frame-to-frame correlation enhances the detection probability, while reducing false alarms due to noise. Thresholding near the peak (say, ~80 percent of the peak) minimizes noise-induced position errors because the signal slope is high. A variable threshold level is probably better, with relative detection level increasing as range to the comet decreases (either semi-automatically or by ground command).

3. DUAL-MODE INSTRUMENT JUSTIFICATIONS

The basic justification for a dual-mode approach navigation/imaging instrument is that it provides adequate performance at minimum cost (including weight and power). Salient points include:

- Use of existing MM '71 television instrument technology.
- Elimination of one camera (wide angle) to reduce cost and complexity.
- Reduction of size and weight of instrument with shorter focal length, while providing adequate resolution.
- Restriction of engineering development primarily to electronics, which is less costly.

4. INSTRUMENT SENSITIVITY

The instrument point source sensitivity is derived from Reference F-2, Figure VIII-24 for the Mariner vidicon, 25μm spot. Limiting star sensitivity (m_v) is related to exposure time (T_e) and aperture (D_o) by:

$$m_v \doteq 2.5 \log (T_e) + 5 \log (D_o) - 1.25; \; T_e \text{ sec}, \; D_o \text{ cm} \qquad (1)$$

For a 33-second exposure time and 6.25-cm aperture (125-mm focal length, f/2.0), $m_v = 6.5$.

The illuminance of a 6.5 magnitude star is 6.1×10^{-10} ft-cd (Reference F-3, page 191) and the vidicon exposure for a 10μm star image diameter and 50 percent optics transmission is 0.36 ft-cd-sec.

5. NAVIGATIONAL STAR FIELD

The average number of stars ($\bar{N}_F$) in a given angular field (Ω_S, sr) of visual magnitude m_v, or brighter, is given by,

$$\bar{N}_F(m_v) = \Omega_S N_o(m_v)/4\pi, \qquad (2)$$

where

$$\log \left[N_o(m_v)\right] = 0.517 \; m_v + 0.599 \qquad (3)$$

Equation 3 is extrapolated from Reference F-4, Table II. The validity of this relationship beyond the tabulation of the Reference ($m_v < 4.4$) is verified by Reference F-5 (page 4) for $m_v < 6.5$ to within about 0.1 percent. For $m_v = 6.5$ and $\Omega_S = 7.5 \times 10^{-3}$ sr (4.4 x 5.6 degrees), $N_o = 9100$ and $\bar{N}_F = 5.4$.

Since the previous number is an average for the entire celestial sphere, it is wise to examine the variations expected for a particular pointing direction. In Reference F-3, page 234, the number of stars brighter than a given photographic magnitude is tabulated as a function of galactic latitude. The number of visual magnitude stars is obtained (approximately) from scaling by the ratio of the mean number of visual and photographic magnitude stars. A few points are summarized in Table 1.

Table 1. Variation of Number of Visual Magnitude Stars with Galactic Latitude

Visual Magnitude,	Number of stars per square degree brighter than m_v at galactic latitude;						
m_v	0°	10°	30°	40°	50°	70°	90°
6.0	.24	.17	.10	.08	.075	.07	.06
7.0	.69	.50	.29	.25	.22	.20	.18
6.5	.44	.31	.18	.145	.135	.13	.11

Thus, for 6.5 visual magnitude and a 4.4 x 5.6 degree field of view (24.6 degree^2), the star field varies between 10-11 stars at the galactic equator to 2-3 stars at the galactic pole. If the instrument pointing direction lies between 30 and 50 degrees galactic latitude during approach guidance, the star field will be three to four stars. This is sufficient to insure identification of a star field, with inputs from the spacecraft attitude control system, and locate the comet with respect to it.

The choice of m = 6.5 as threshold sensitivity of the image system means that the comet could be acquired onboard the spacecraft at a range of about $6 \cdot 10^6$ km in accordance with the photometric model discussed in Section 2.7.4, Volume I (see Figure 2-27 in particular). The threshold detection feature reduces the comet's image size from the estimated angle of about 1 degree at this range to less than 1 arc minute without significant loss in total brightness. This in turn permits more accurate initial navigation fixes with respect to the reference stars. The preferred navigation mode discussed in Section 5 actually does not require accurate fixes until the range is less than 10^6 km when the nucleus is brighter than m = 4. Thus the sensitivity threshold is not so much dictated by early comet acquisition but by the necessity of acquiring a sufficient number of reference stars.

5. OPTICS RESOLUTION

The point source resolution of the instrument is assumed to be the same as Mariner (10 μm), even though the angular field has been increased by a factor of four and the focal ratio changed to 2.0 from 2.4. This is justified by the following analysis.

The spot size for a diffraction-limited optical system or relative aperture, f/2.0 at 0.55 μm is 2.7 μm. A Schmidt optical system is theoretically diffraction limited on axis and degrades off-axis according to Reference F-6, page 394.

$$d(\text{Schmidt}) = f\,\phi^2/(24\,F^3) \qquad (4)$$

f = focal length

ϕ = off-axis angle

F = focal ratio

For this 125-mm, f/2.0 optical system, d(Schmidt) = 2.6 μm at the maximum off-axis angle (3.6 degrees). The sum of these spot diameters is 5.3 μm, so that the optical system is realizable, particularly since performance will not significantly degrade until the spot diameter exceeds the vidicon beam size (~25 μm).

6. INSTRUMENT RESOLUTION

The instrument sensor is the same slow scan vidicon employed in the Mariner 1969 and 1971 cameras. An active raster size of 12.5×9.6 mm^2 is used, with 700-scan lines and 832 pixels/line in a 42-second frame.

With optics of 125 mm focal length, the total field coverage is 4.4×5.6 degrees. Thus, each pixel represents an angular resolution of 0.12 mrad. Calibration of the instrument should allow estimation of the comet nucleus (center of brightness) direction with respect to the known star field to an accuracy of 0.25 mrad (3σ).

Resolution is dependent on image smear. For an allowable image smear of one pixel (0.12 mrad), a 33-second exposure time requires a

maximum spacecraft limit cycle rate of 0.0002 degree/second, which is realizable.* At closer approach, relative motion of the comet with respect to the spacecraft will necessitate shorter exposure times, either by varying the mechanical shutter speed or by employing adjustable vidicon beam blanking. The loss of sensitivity with shorter exposure time will be offset by increased comet brightness at the closer ranges.

REFERENCES

F-1 NASA TM 33-505, "Development and Testing of the Television Instrument for the Mariner Mars 1971 Spacecraft," JPL, Pasadena, California, 1 November 1971.

F-2 Study of Comet D'Arrest probe, JPL report 760-66.

F-3 Allen, C. W., Astrophysical Quantities, Second Edition, The Athlone Press, 1963.

F-4 Kleiman, L. A. and Arehart, R. A., "An Analytical Approach to the Determination of Stellar Fields of View," NASA TR R-257, June 1967.

F-5 Yale University Observatory, Catalogue of Bright Stars, Third Revised Edition, 1964.

F-6 Smith, W.J., Modern Optical Engineering, McGraw-Hill, 1966.

*See also Section 5.5.5, Volume I

APPENDIX G

ELECTROSTATIC EQUILIBRATION OF A SPACRAFT CARRYING ION ENGINES

For a spacecraft carrying ion engines and moving in the cometary environment, both active and passive modes of electrical equilibration are possible. The passive mode of electrical equilibration is obtained when all portions of the thrust system are turned off. In this mode the electrical potential of the spacecraft relative to the surrounding cometary plasma is determined by the flux of space plasma particles upon the spacecraft surface and by the photo-current of electrons emitted by the spacecraft under the action of the solar UV. It is important to note that passive spacecraft equilibration is, in the vast majority of conditions, a state of electrical contamination (non-zero surface electric field). This electrostatic contamination alters the energy and directionality of low energy particles in the cometary plasma. In addition, if the cometary plasma is very tenuous as is expected, then the equilibration potential of the spacecraft relative to the plasma will be positive, and photo-electrons from the spacecraft surface will remain in the near vicinity creating a contamination of the cometary plasma electron population. In summary, passive equilibration of a spacecraft in a dilute space plasma leads to electrostatic contamination that affects low energy particle energy and directionality measurements and produces space plasma electron contamination by trapped photo-electrons from the spacecraft surface.

Operation of the ion thruster(s) places the spacecraft in a state of active equilibration. Here the spacecraft potential relative to the cometary plasma will be determined by the coupling of the exhaust beam plasma to the space plasma, by the injection potential of electrons from the neutralizer to the thrust beam, and by the bias of the neutralizer relative to the spacecraft. In this discussion we assume that the neutralizer is closely coupled to the thrust beam with an injection potential of 10 volts or less. Under these conditions spacecraft electrostatic cleanliness can be achieved. In practice this requires the use of an E-meter (a device which measures the spacecraft surface electric field), certain feedback circuitry, and a variable bias voltage between the

neutralizer and the spacecraft. The E-meter signal causes the neutralizer bias voltage to vary until the spacecraft surface electric field vanishes. This condition of electrostatic cleanliness allows low energy charged particles in the cometary plasma to reach the particle detectors in the scientific payload without perturbations to either their energy or directionality.

A possible interference with science payload operation caused by the operation of the ion thruster is in space plasma contamination — specifically in a contamination in the space plasma electrons. This process of space plasma contamination may occur under conditions of spacecraft electrostatic cleanliness. The space plasma electrons and thrust beam electrons may interchange along the entire boundary where these two plasmas meet. "Outwardly" diffusing thrust beam electrons interchange with "inwardly" diffusing space plasma electrons. The thrust beam electrons entering the space plasma would not normally move into the regions on the spacecraft where the particle detectors are located if the magnetic field $\vec{B}$ were perfectly zero. Actually, the space magnetic field is not zero, but may be of the order of several γ ($1\gamma = 10^{-5}$ gauss). These weak fields bend the trajectories of low energy electrons so that a thrust beam electron entering the space plasma at the "rear" of the spacecraft may move in a circle (whose radius may be many meters) and encounters the particle detectors at the front. A key factor in this process is the quality of the beam neutralization. Effective neutralization, i.e., low injection potential, reduces space plasma contamination and makes the condition of spacecraft electrostatic cleanliness easier to obtain.

While the "thruster on full" condition leads to the more easily programmable active equilibration, several other alternatives are possible. These may be described as "partial thruster," "thruster off-neutralizer on," and "thruster off-extractors on." In the "partial thruster" active equilibration mode a reduced level of thrust beam plasma continues to be directed into the space plasma. This condition does not produce appreciable thrust, but does lead to sufficient plasma densities to couple the thrust beam plasma effectively to the space plasma. Active electrical equilibration of the spacecraft via the bond of the thrust beam-space plasma is still possible. The mode utilizes less thruster power and,

possibly, reduced levels of space plasma contamination will result. An unknown aspect of this mode is the quality of the neutralizer-thrust beam coupling as the beam plasma density diminishes. For the mercury discharge neutralizer, which is the most likely means of beam neutralization to be used, primary attention has been focused on beam coupling under full loads. Retention of strong beam-neutralizer coupling under partial beam loads must be demonstrated.

Another mode of active equilibration is "thruster off-neutralizer on." Here the thruster system is turned off completely but power remains on the discharge neutralizer. By possible arrangement of the "keeper" voltages on the discharge neutralizer it may be possible to eject either ions or electrons from the neutralizer into space. The release of electrons is, in general, not likely to be the required equilibration action, since the spacecraft photo electric emission is probably larger than the space plasma electron diffusion current. However, the release of a comparatively small current of ions from the discharge neutralizer to space would allow the spacecraft equilibration potential to move in a negative direction and, thus, reduce the difference in potential between the spacecraft and the space plasma. The advantages of the "neutralizer equilibration" mode are a very low power requirement and almost negligible space plasma contamination; i.e., the trajectory of ions released will not be bent by the space magnetic field sufficiently to reach the spacecraft area where particle detectors are located. The E-field meter, feedback circuitry, and variable neutralizer bias voltages discussed in the "thruster on full" mode are equally applicable for this mode. To achieve electrostatic cleanliness, however, will probably require a different feedback logic for the "neutralizer equilibration" mode.

A final active mode of equilibration to be considered here is "thruster off-extractors on." Here the thrust system is completely off and active equilibration of the spacecraft is achieved by biased extractor electrodes placed in the space plasma. For a sunlit spacecraft in a very dilute plasma the emitted photo-electron current generally exceeds the electron diffusion currents from the space plasma. If a positive bias potential is placed on an extractor electrode in contact with the space plasma an additional current of electrons is drawn to this electrode. By sufficient

increases in this electrode bias potential, electron drainage current occurs from a large region of space, and arriving electrons begin to approach the number of photo-electrons attempting to leave the spacecraft. Electrostatic cleanliness is achieved when all electron currents are exactly in balance, and the spacecraft equilibration potential is zero. Space plasma ion currents have been neglected in this discussion since these particle flows are small compared to the magnitudes of the electron currents. This equilibration method is simple and required power is at very low levels. An E-field meter and feedback circuitry are needed to maintain electrostatic cleanliness. Since the extractor sheath region may become very large in a dilute plasma it is required that the extractor be mounted on a long boom or on the tip of the solar array to prevent the sheath region from extending to the particle detectors location. The feedback circuits that control the equilibration must have an extremely short time contact since electron collection times (period required for an electron to move from the plasma to the extractor) and emission times (period required for emitted electron to move to the space plasma) are very short.

Work on advanced concepts of SEP spacecraft equilibration and plasma interactions was performed by TRW under JPL contract. The results are reported in detail in References G-1 and G-2.

REFERENCES

G-1 "Study of Electric Spacecraft Plasmas and Field Interactions," Robert K. Cole, H. S. Ogawa, and J. M. Sellen, Jr., TRW Document 07677-6013-R000, May 1, 1968.

G-2 "Study of Electric Propulsion Spacecraft Plasmas and Field Interactions," Robert K. Cole, H. S. Ogawa, and J. M. Sellen, Jr., TRW Document 12738-6017-R00-00, July 1, 1970.

APPENDIX H

EFFECT OF 1980 COMET FLYBY DATA ON ASSEMBLY AND TEST OF 1984 RENDEZVOUS SPACECRAFT

As discussed in Sections 1 and 5, we assume that comet data will become available from the 1980 flyby mission that could require changes in the rendezvous mission spacecraft at a time when it is in the process of assembly and test. The type and extent of possible changes are affected by the time remaining to make the changes before delivery of the spacecraft to the launch site. As the spacecraft approaches the launch date, there is a point in time when no changes can be made without significantly delaying the launch date.

Consideration is given here to two cases, one where the data is available five months prior to launch, and the other, where it is available 17 months prior to launch. In the analysis of both cases, an SEP spacecraft development plan derived in a previous TRW study (Reference 1-6) was used as a representative schedule for spacecraft manufacturing and integration operations. Case A (five months), and Case B (17 months) are each superimposed on the schedule to pin point the spacecraft operations that are in process at each point in time, see Figure H-1.

Option A

If the data is received and changes are initiated five months prior to launch, the spacecraft is at this time completely assembled and it is entering the final environmental tests. Because of this condition, any change would have to be quite simple so as not to require retest of the entire spacecraft. The changes that can be made include:

1) "Screwdriver" adjustments without any removals.

2) Replacement of complete units with other complete units that are identical in size, weight, c.g. location, power requirement, thermal response, etc. Typically, this type of change includes sensors, detectors, and whole units. To effect this type of change a second set of units must be provided in advance for each change that is anticipated.

3) Alteration of computer programs or the in-flight guidance program.

FOLDOUT FRAME 1

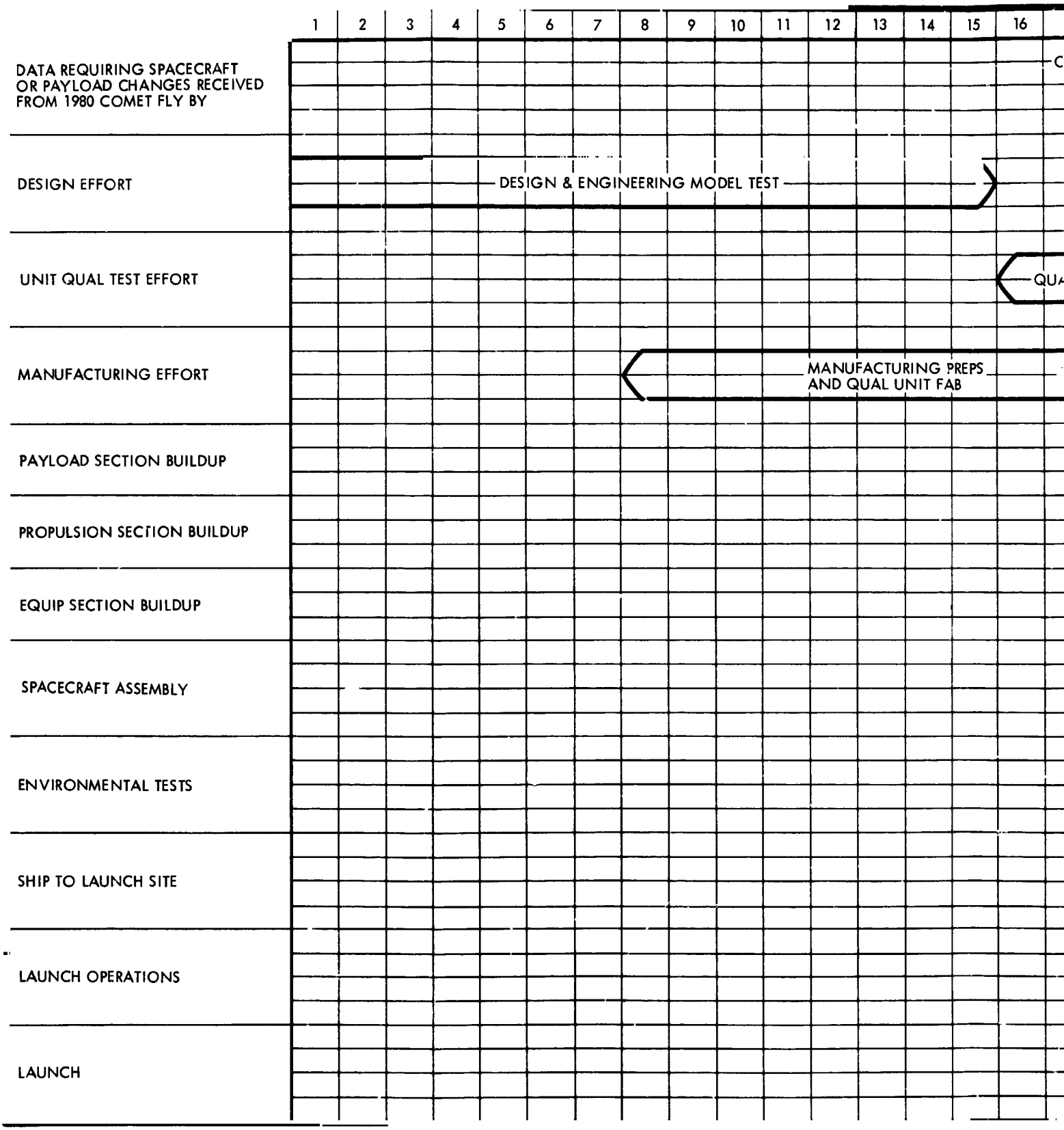

Figure H-1. Effect of Comet Data on Spacecraft Development

FOLDOUT FRAME 2

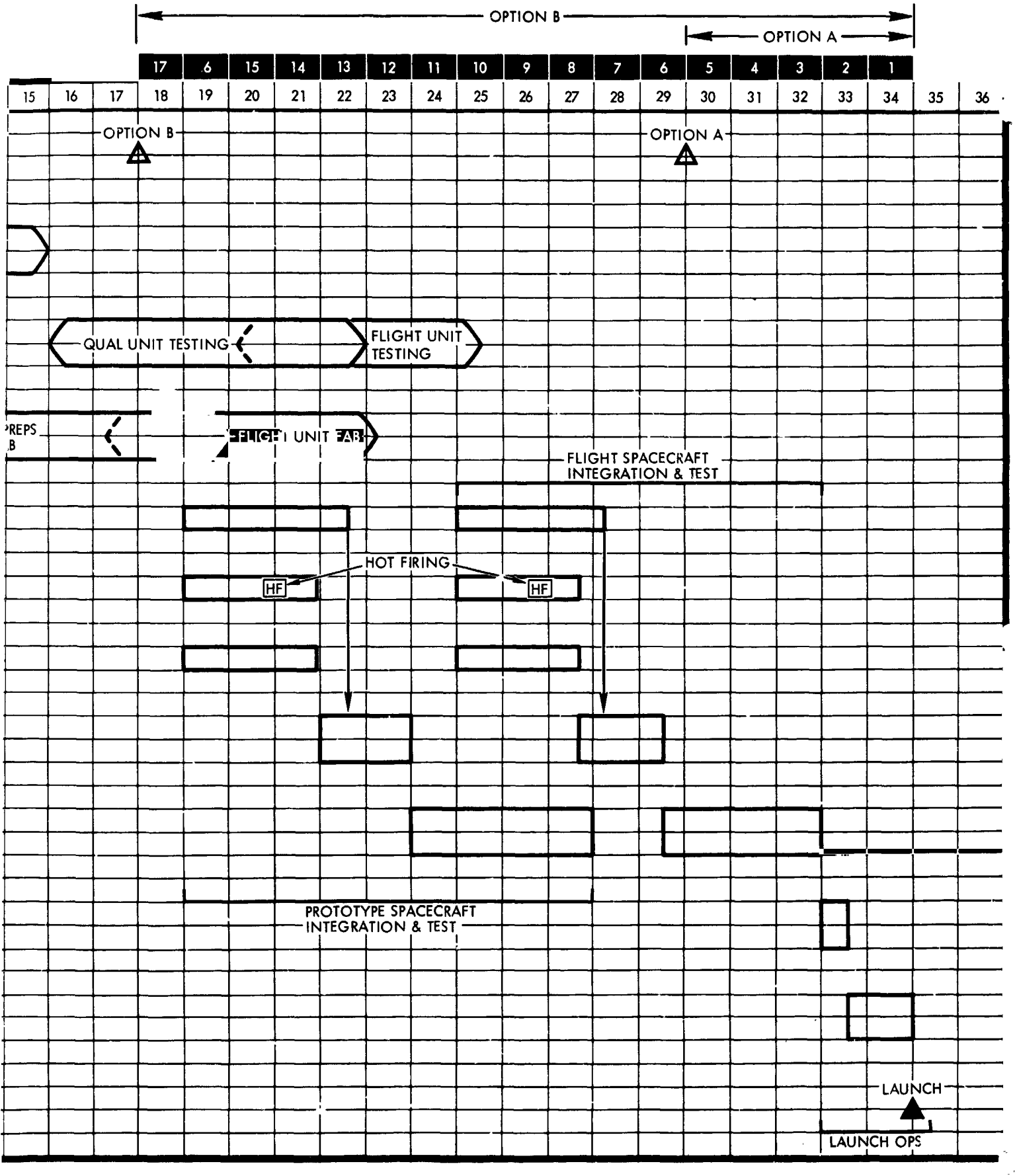

These changes must be designed into the spacecraft and the hardware tested and ready for quick installation. The changes that are possible are also affected by how quickly the flyby data is evaluated and a decision is made to make the change. This time is subtracted from the five months and only three months are available prior to shipment to the launch site. Therefore, it is very desirable to prepare the changes carefully and make the decision expeditiously.

Option B

In this case, the data is received during the period when the units for the flight spacecraft are still in manufacturing, and flight acceptance test has not begun. A period of three months remains before a flight unit acceptance test start so that there is a possibility of incorporating the change without having to disassemble the unit. However, even if the unit is assembled, the rework and retest of a completed unit nominally requiring four to five weeks can be done "off line" without disturbing the main schedule. This type of change can be made up to ten months from launch without appreciable impact on the development program.

Both options, of course, would cause an increase in cost, with Option A obviously being more expensive because of the additional hardware required and the extra design and planning effort to fully anticipate the possible changes. The cost, in the case of Option B, is increased only by the additional hardware at the piece part level and the extra effort for rework.

APPENDIX I

SUMMARY OF TECHNICAL INNOVATIONS

The following list summarizes technical innovations in mission and spacecraft design, that were conceived under this study contract. This list is submitted in compliance with the New Technology Reporting Clause called out in the study contract. A more complete discussions will be submitted by TRW Systems in a separate document.

The possibility of a transfer to the commercial sector of these innovations which are related specifically to interplanetary missions appears to be remote.

1) Two-Stage Rendezvous. The two-stage comet rendezvous mode reduces the required accuracy of approach navigation, thus simplifying the onboard navigation instrument, and saves thrust time and propellant expenditure during the initial coma exploration. (Section 5.5.4)

2) Thermal Protection Behind Nucleus. Hovering in the penumbra of the comet's nucleus for an extended time (20 days or more) provides effective thermal protection of the spacecraft. However this mode entails loss of mobility for comet exploration and requires intermittent stationkeeping thrust typically for a short period every day. This mode is introduced as a possible emergency measure during the hottest part of the mission. (Section 5.4.3)

3) Probing of Solar Wind Phenomena. Repeated comet exit and entry maneuvers are useful for comparison of plasma interactions inside the comet envelope with the undisturbed solar wind outside. A total comet exploration period of 80 to 100 days gives time for such maneuvers. (Section 6.9)

   The possible use of a small, spin-stabilized deployable probe as a solar wind monitor that would relay its observations to earth via the mother spacecraft is an attractive alternative but has been excluded from the current basic mission concept in the interest of simplicity and cost economy. (Section 6.8.3)

4) Circumnavigation Maneuvers. Circumnavigation of the nucleus requires intermittent radially inward directed thrust. This is facilitated by slow rotation of the

spacecraft in the plane of its motion around the nucleus, and repeated discrete reorientation maneuvers are made unnecessary. (Section 6.6.2)

5) Simplified Graphical Analysis of Relative Comet, Earth, and Sun Positions. A "bipolar" plot of the comet's relative trajectory can be used for convenient graphical analysis of range and view angles from earth to comet and spacecraft and vice versa. This trajectory is invariant with the year of the comet's apparition. Apparent comet magnitudes and times of acquisition by earth can be readily determined with the aid of this plot. (Appendix A)

6) Thrust-While-Hover Nucleus Gravity Measurement. Hovering at close distance to the nucleus permits gravity measurement through on-off thrust application so as to maintain a fixed average altitude. Altitude feedback by an altimeter radar is required. Since gas flow from the nucleus adds a perturbing force, the effect of gravity and gas flow pressure can be separated through variations of the solar array angle, or partial retraction. Determination of the gas flux is a desirable by-product of this technique. (Section 6.6.3)

7) Orbital Test Capabilities Provided by Shuttle Launch. If the solar-electric spacecraft is to be launched by a Shuttle/upper stage combination, it will be advantageous to perform an orbital preflight test of the solar arrays and the electric propulsion system. A complete system test with fully deployed solar arrays and ion engines operating is not practical on the ground. Service and repair functions could be performed by the Shuttle crew in case of malfunction, or the spacecraft returned to the ground. (Section 7.5)

8) Solar Array Panel Stiffening to Control Edge Curl. Stiffener tubes mounted crosswise and along the edges of the solar array blankets serve to avoid harmful curling of the blankets under extreme thermal flux. The prestressed collapsible tubes of the type developed by Ryan Aeronautical Engineering and TRW Systems as deployment booms flatten against the solar array substrate during stowage on the rollup drums and add a weight penalty of only about four percent. (Section 7.3.3)

APPENDIX J

MODERN OBSERVATIONS OF P/ENCKE EXTRACTED FROM VSEKHSVYATSKII'S COMPILATION

A major source of historical data on comets is the formidable compilation by S. K. Vsekhsvyatskii, "Physical Characteristics of Comets" (reference list Section 2). The book contains statistical, parametric, theoretical, descriptive, graphic, and photographic information on cometary observations from 466 B. C. to 1957 A. D. In addition, two supplements have been published, covering data obtained through 1965, but without the extensive descriptive material in the book.

Many numerical values and qualitative assessments of cometary features derived from past observations, especially magnitudes and identifications of cometary nuclei, must be regarded with appropriate skepticism by contemporary astronomers. Nevertheless, the data have served many researchers as a departure from which to pursue their investigations and have been liberally used as background and source material for parts of the present report. Part Three of Vsekhsvyatskii gives a chronological list of all cometary observations, largely in narrative form and with a structure not always convenient for rapid assimilation of readers of this report. The following pages reproduce the Explanatory Notes and Bibliographic Abbreviations for Part Three and the relatively modern entries for Encke only, beginning with the perihelion passage of 1885 that opened the second, and present, century of Encke's recorded history.*

*This excerpt is from the NASA-sponsored English translation (1964), NASA TT F-80, Office of Technical Services OTS 62 11103, of Vsekhsvyatskii's work.

Part Three

OBSERVATIONS AND PHYSICAL CHARACTERISTICS

Explanatory Notes

In this main part of the book the cometary apparitions are reviewed one by one, and data given on the apparent motion, observed distinctive features and dimensions, and the brightness. A short account of observations is followed by references to the original investigations of the physical characteristics. While no claim is made to an exhaustive treatment, the data brought together here should suffice to provide a basis for future research. The Kiev Observatory Library provided most of the material used here, with occasional reference to the libraries of the Astronomical Institute im. Shternberg, and of the Moscow State University and Pulkovo Observatories.

The account of each apparition is presented according to the same scheme: date and circumstances of discovery; a brief description of the comet's heavenly itinerary (these enable one to make a rough reconstruction of the visibility conditions at the various localities of observation); specific estimates of physical characteristics, mainly brightness, head diameter, and tail length; and a description of variations in appearance during the period of visibility.

For the faint comets observed during the eighteenth and nineteenth centuries photometric estimates are almost entirely lacking. The total magnitude in these cases was estimated, following Holetschek, from descriptions of the object's appearance during position determinations, allowing for conditions of visibility (cloudiness and transparency, position of the Moon, background brightness, the kind of instrument used, elevation of the comet above the horizon, etc.). Independent estimates based on descriptions by different observers show that the error is generally less than 1 to 2^m.

An attempt was made to establish criteria for determining the apparent brightness or, to be precise, upper and lower limits for it, from the estimated head diameter, the kind of instrument and the magnification used. Such formal relations leave out the effect of the prevailing conditions of visibility, and with this qualification the following criteria were set up:

1. The total brightness of a comet barely made out with the naked eye on a clear moonless night with no twilight must have been at least $5^m.5$.
2. The brightness of a comet observed for position determination through a 4-inch meridian circle must have been at least $7\text{-}8^m$.
3. A comet seen through a 3-inch telescope could not be fainter than 9^m.
4. A comet bright enough to have had its position determined through a 10-inch refractor with filar micrometer, provided its diameter was >2', could not be fainter than 10 to $10^m.5$.

It is established beyond any doubt that nineteenth-century observers consistently underestimated apparent brightness, because in their position determinations they only referred to the central condensation.

Next, under References are given the main reports on observations of physical features. This is followed by the name of the computer of the orbit and the appropriate reference.

The next paragraph concisely reviews the determinations of the absolute magnitude and other photometric parameters. The value of the reduced head diameter D_1 (corresponding to $\Delta = 1$ a. u.) is now given, averaged over a certain time interval, as obtained from the apparent diameter D

$$D_1 = D\Delta.$$

Both D and D_1 are given in minutes of arc. To convert into kilometers multiply D_1 by 44,000.

If there was a tail, its maximum length S is given, like Holetschek did, in a. u. One readily verifies that

$$S = \frac{\sin c}{\sin (k-c)},$$

where c is the apparent angular span of the tail, and k the phase angle (subtended by Earth and Sun at the nucleus). Obviously

$$\cos k = \frac{r^2 + \Delta^2 - R^2}{2r\Delta},$$

where r, Δ are the comet's helio- and geocentric distances, and R the Earth-Sun distance. Alternatively,

$$\tan^2 \frac{k}{2} = \frac{(p-r)(p-\Delta)}{p(p-R)}; \quad p = \frac{1}{2}(r + \Delta + R)$$

The account ends with notes on special investigations: determinations of tail type, association with meteors, spectra, etc., with pertinent references.

Bringing up the rear for each apparition are r and Δ values for various dates, which in the majority of cases were obtained from ephemerides and

Class	Definition		Number of objects	Mean magnitude
	Brightness	Diameter		
I	extremely faint	3-4"	251	$10^m.9$
II	very faint	10-12"	108	10.9
III	quite faint	20-30"	6	11.4 (?)
IV	faint	20-30"	28	9.8
V	somewhat faint	50-60"	17	9.9
VI	appreciably bright	50-60"	18	9.0
VII	rather bright	3-4'	-	-
VIII	bright	3-4'	-	-
IX	very bright	8-10'	-	-
X	uncommonly bright	>20'	-	-

as such their accuracy occasionally leaves much to be desired. They are given to within 0.01 a. u. over the entire period of observations and may be used for rough computations.

In some cases (e. g., Comet 1879 III) W. Herschel's classes are cited (also used by J. Herschel) which grade the brightness and size of nebulae and star clusters. Their definitions are reproduced above from the NGC, as given by Dreyer. To this we append the distribution of objects in Holetschek's catalogue* according to those classes and the mean magnitude based on the data of that catalogue. The scatter in magnitudes within each class is considerable (they range from 9 to 12^m in Class I). Holetschek's magnitude scale corresponds closely that of the BD.

* Holetschek, J. -Wien Stw. Ann., 20: 114-119. 1907.

Bibliographic Abbreviations

Individual publications

Baldet and de Obaldia. Baldet, F. and G. de Obaldia. Catalogue général des orbites de comètes de l'an -466 à 1952. Paris. 1952.

Biot. Biot, E. Catalogue des comètes observées en Chine depuis l'an 1230 jusqu'à l'an 1640 de notre ère. Also, Catalogue des etoiles extraordinaires observées and Chine, depuis les temps anciens jusqu'à l'an 1203 de notre ère. — C. d. T. 1846.

Holetschek. Holetschek, J. Untersuchungen über die Grösse und Helligkeit der Kometen und ihrer Schweife. Vienna. 1896-1917:—
Part I (up to Comet 1759 III). — Denksch. Wiener Ak., Math. Naturwiss. Kl., 63: 317. 1896;
Part II (comets from 1762 to 1799). — ibid., 77: 503. 1905;
Part III (comets from 1801 to 1835). — ibid., 88: 745. 1913;
Part IV (bright periodic comets). — ibid., 93: 201. 1916;
Part V (fainter periodic comets). — ibid., 94: 375. 1917.

Pingré. Pingré, P. Cometographie ou traité historique et théorique des comètes. Paris. Vol. I, 1783; Vol. II, 1784.

Williams. Williams, J. Observations of Comets, from B. C. 611 to A. D. 1640. Extracted from the Chinese Annals. London. 1871.

V. I. Vsekhsvyatskii, S. K. On the Brightness of Comets [in English]. — A. Zh., 2: 68 [no year given].

C. A. M. Vsekhsvyatskii, S. K. General Catalogue of the Absolute Magnitudes of Comets [in English]. — A. Zh., 10(3): 327. 1933. (442 apparitions).

E-I. Vsekhsvyatskii, S.K. Extension of the C. A. M., I. Comets of 1919-1934. [See above; in English]. — A. Zh., 12(3): 243. 1935. (36 apparitions).

E-II. Vsekhsvyatskii, S. K. Extension of the C. A. M., II. Comets of 1849-1880. [In English]. — A. Zh., 14(5-6): 480. 1937.

E-III. Vsekhsvyatskii, S. K. Yarkost' komet 1880-1900 gg. i nekotorye osobennosti raspredeleniya absolyutnykh velichin komet (The Brightness of Comets 1880-1900 and Some Features of the Distribution of Cometary Absolute Magnitudes). — A. Zh., 25(6): 337. 1948; also, Dopolnenie k katalogu absolyutnykh velichin komet III (Extension of the C. A. M., III). — Publ. Kiev Obs., No. 2: 93. 1948. (41 apparitions).

E-IV. Konopleva, V. P. Dopolnenie k obshchemu katalogu absolyutnykh velichin S. Vsekhsvyatskogo IV. Komety 1934-1946 (Extension of S. Vsekhsvyatskii's C. A. M., IV. Comets of 1934-1946). — Publ. Kiev. Obs., No. 3: 55. 1950.

E-V. Vodop'yanova, T. V. Absolyutnye velichiny komet 1947-1954 (Absolute Magnitudes for Comets of 1947-1954). — Astr. Tsirk., 145: 15. 1954; 147: 16. 1954; 150: 11. 1954; 169: 22. 1956.

Periodicals

Abh. A. N. Astronomische Abhandlungen der Astronomischen Nachrichten.

Abh. Schwed. Akad. Abhandlungen der Schwedischen Akademie der Wissenschaften.

Acta Astr. Acta Astronomica.

Acta Petr. Acta Petropolitana [St. Petersburg].

A. J. Astronomical Journal.

A. Jb. Astronomischer Jahresbericht.

Allg. Geogr. Eph. Allgemeine Geographische Ephemeriden.

Ame J. Sci. American Journal of Science.

A. N. Astronomische Nachrichten.

Ann. Aph. Annales de l'astrophysique.

Ann. Bordeaux. Annales de l'Observatoire de Bordeaux.

Ann. de Belgique. Annales de l'Academie de Belgique.

Ann. de Bur. Long. Annuaire du Bureau des Longitudes.

Ann. Meudon. Annales de l'Observatoire de Meudon.

Ann. Mosc. Obs. Annales de l'Observatoire de Moscou.

Ann. Obs. Venezia. Annales de l'Observatoire de Venezia.

Ann. Obs. Paris. Annales de l'Observatoire de Paris.

Ann. Sci. Annals of Science.

Ann. Tokyo Obs. Annals of the Tokyo Observatory.

Ap. J. Astrophysical Journal.

Arch. Sci. Phys. Nat. Archives des sciences physiques et naturelles.

Argelander Obs. Argelander Observationen.

Astr. a. Aph. Astronomy and Astrophysics.

Astr. Tsirk. Astronomicheskii Tsirkulyar Byuro Astronomicheskikh Soobshchenii AN SSSR (Astronomical Circular of the Bureau of Astronomical Information of the USSR Academy of Sciences).

Atti Acc. Lincei. Atti della Accademia Royale dei Lincei.

A. Zh. Astronomicheskii Zhurnal (Astronomical Journal of the USSR).

B. A. Bulletin astronomique.

B. A. A. Hbk. British Astronomical Association Handbook.

B. A. A. J. Journal of the British Astronomical Association.

B. A. A. Mem. Memoires of the British Astronomical Association.

B. A. N. Bulletin of the Astronomical Institutes of the Netherlands.

Bergedorf Mitt. Bergedorf Mitteilungen.

Berl. Ast. Jahrb. Berliner astronomisches Jahrbuch.

Berlin Beob. Berliner Beobachtungen.

Bothkamp Beob. Bothkamp Beobachtungen.

Brünnows Astr. Not. Brünnows astronomische Notizen.

B. S. A. F. L'Astronomie et bulletin de la société astronomique de France.

Bull. Acad. Belgique. Bulletin de l'Academie de Belgique.

Bull. Acad. Petersburg. Bulletin physique et mathematique de l'Academie de St. Petersburg.

Bull. Belgrade. Bulletin de l'Observatoire de Belgrade.

Bull. Hebdomad. Bulletin hebdomadaire.

Bull. Inst. Teor. Astr. Byulleten' Instituta Teoreticheskoi Astronomii (Bulletin of the Institute for Theoretical Astronomy [Leningrad]).

Bull. KISO. Byulleten' Komissii po Issledovaniyu Solntsa (Bulletin of the Solar Research Commission).

Bull. Madrid. Bulletin de l'Observatoire de Madrid.

Bull. Obs. Géneve. Bulletin de l'Observatoire de Génève.

Bull. Obs. Paris. Bulletin astronomique de l'Observatoire de Paris.

Bull. Obs. Soc. Byulleten' Obshchestva Nablyudatelei (Bulletin of the Observers' Society).

Bull. Poulkovo. Bulletin de l'Observatoire de Poulkovo.

Bull. Soc. Moscou. Bulletin de la société de science de Moscou.

Bull. Soc. Observers Moscow. Byulleten' Kollektiva Nablyudatelei, Moskva (Bulletin of the Moscow Observers' Association).

Bull. Stalinabad. Obs. Byulleten' Stalinabadskoi Observatorii (Bulletin of the Stalinabad Observatory).

Bull. Wilna. Bulletin de l'Observatoire de Wilna.

B. Z. Beobachtung-Zirkular der astronomischen Nachrichten.

Cambridge Obs. Cambridge Observations.

Cape Ann. Annals of The Cape Observatory.

C. d. T. Connaissance des temps.

Cincinnati Obs. Cincinnati Observations.

Circ. Pulkovo Obs. Circular of the Pulkovo Observatory.

Cooper Obs. Cooper Observations.

Corr. Astr. Correspondance astronomique.

C. R. Comptes rendus de l'Academie des Sciences (Paris).

Dokl. Akad. Nauk. Doklady Akademii Nauk SSSR (Proceedings of the USSR Academy of Sciences).

Dominion Obs. Ap. J. Dominion Observatory Astrophysical Journal.

Dorpat Beob. Dorpat Beobachtungen.

Dorpat Obs. Dorpat Observationen.

Denksch. Wiener Ak. Denkschriften der Wiener Akademie.

Edinburgh J. Sci. Edinburgh Journal of Science.

Ergänz. Heft. Ergänzungsheft zu den Astronomischen Nachrichten.

GAO. Glavnaya Astronomicheskaya Observatoriya (Main Astronomical Observatory [of the USSR Academy of Sciences, at Pulkovo]).

Greenwich Obs. Greenwich Observations.

H. A. C. Harvard Announcement Cards.

Harvard Ann. Annals of the Harvard Observatory.

Harvard Bull. Bulletin of the Harvard Observatory.

Harvard Circ. Circular of the Harvard Observatory.

Hind. Mag. Hindenburg's Magazine.

I. A. U. C. International Astronomical Union Circular.

Izv. AN. Izvestiya Akademii Nauk (Reports of the USSR Academy of Sciences).

Izv. Krym. Obs. Izvestiya Krymskoi Observatorii (Reports of the Crimean Observatory).

Izv. Odess. Obs. Izvestiya Observatorii Odesskogo Universiteta (Reports of the Odessa University Observatory).

Izv. Pulkov. Obs. Izvestiya Pulkovskoi Observatorii (Reports of the Pulkovo Observatory).

Izv. RAO. Izvestiya Russkogo Astronomicheskogo Obshchestva (Reports of the Russian Astronomical Society).

Japan J. Astr. Geoph. Japanese Journal of Astronomy and Geophysics.

J. Astr. Soc. S. Africa. Journal of the Astronomical Society of South Africa.

J. Obs. Journal des observateurs (Marseilles).

J. Phys. Rad. Journal de physique et de radium.

J. Shanghai Sc. Inst. Journal of the Shanghai Institute of Science.

Königsberg Beob. Königsberg Beobachtungen.

Königsberg Obs. Königsberg Observationen.

Kwasan Bull. Bulletin of the Kwasan Observatory.

Lalande Bibl. Lalande bibliographie.

Lesgaft Inst. Trudy Instituta im. Lesgafta (Reports of the Institute im. Lesgaft).

Leyton Obs. Leyton Observations.

L. O. B. Lick Observatory Bulletin.

Lockyer Obs. Bull. Bulletin of the Lockyer Observatory.

Lowell Obs. Bull. Bulletin of the Lowell Observatory.

Maskelyne Obs. Maskelyne Observations.

M. Corr. Monatliche Correspondenz für Erd- und Himmelkunde (Burkhardt's).

Mém. Acad. Paris. Mémoires de l'Academie de Paris.

Mém. Acad. Petersburg. Mémoires de l'Academie de St. Petersburg.

Mém. de Géneve. Mémoires de l'Academie de Génève.

Mém. de l'Inst. Mémoires de l'Institute.

Mem. Japan. Astr. Ass. Memoirs of the Japanese Astronomical Association.

Mem. R. A. S. Memoirs of the Royal Astronomical Society (London).

Mem. Soc. Astr. It. Memoire della Società Astronomica Italiana.

Mem. Spec. It. Memoire della Società degli Spectroscopisti Italiani.

Mitt. Hamburg Stw. Mitteilungen der Hamburger Sternwarte.

Mitt. Pulkovo. Mitteilungen der Pulkovo Sternwarte.

Mitt. Wien Stw. Mitteilungen der Wiener Sternwarte.

M. N. Monthly Notices of the Royal Astronomical Society (London).

Obs. The Observatory.

Obs. Paris. Les observations astronomiques de Paris.

P. A. S. P. Publications of the Astronomical Society of the Pacific.

Perkins Obs. Contr. Contributions from the Perkins Observatory.

Phil. Trans. Philosophical Transactions of the Royal Society.

Pop. Astr. Popular Astronomy.

Poznan Obs. Poznan Observations.

Proc. Amer. Acad. Proceedings of the American Academy.

Proc. Roy. Soc. Proceedings of the Royal Society.

Proc. Tokyo Acad. Proceedings of the Tokyo Academy.

Publ. A. A. S. Publications of the American Astronomical Society.

Publ. Copenh. Obs. Publications of the Copenhagen Observatory.

Publ. Inst. Astr. Varsovie. Publications de l'Institute astronomique de Varsovie.

Publ. Bishop's Obs. Publications of the Bishop's Observatory.

Publ. Heidelberg. Stw. Publicationen der Heidelberger Sternwarte

Publ. Jurjew Stw. Jurjew Sternwarte Publicationen.

Publ. Karlsruhe Stw. Publicationen der Karlsruhe Sternwarte.

Publ. Kazan. Obs. Publikatsii Kazanskoi Observatorii (Publications of the Kazan Observatory).

Publ. Kharkov. Obs. Publikatsii Khar'kovskoi Observatorii (Publications of the Khar'kov Observatory).

Publ. Kiel Obs. Kiel Sternwarte Publicationen.

Publ. Kiev. Obs. Publikatsii Kievskoi observatorii (Publications of the Kiev Observatory).

Publ. Kuffner Obs. Publicationen der Kuffner Sternwarte.

Publ. Lick Obs. Publications of the Lick Observatory.

Publ. Michigan. Michigan Observatory Publications.

Publ. Obs. Warsaw Univ. Publications of the Warsaw University Observatory.

Publ. Oss. Milano. Publicatione della osservatorio di Milano.

Publ. Pulkov. Obs. Publikatsii Pulkovskoi Observatorii (Publications of the Pulkovo Observatory).

Publ. Tartu. Obs. Publikatsii Tartuskoi Observatorii (Publications of the Tartu Observatory).

Publ. Yerkes Obs. Publications of the Yerkes Observatory.

Rend. Roy. Acad. It. Rendiconti della Royale Accademia Italiana dei Lincei.

Rev. de Espana. Revista de la sociedad astronomica de España y America.

Russ. A. J. Russkii Astronomicheskii Zhurnal (Russian Astronomical Journal).

Sitz. Akad. Wien. Sitzungsberichte der Kaiserlichen Akademie in Wien.

Sky a. Tel. Sky and Telescope.

Stockholm Ann. Stockholm Annalen.

Strassburg Circ. Circular der Sternwarte Strassburg.

Trans. Yale Obs. Transactions of the Yale Observatory.

Trudy Astr. Obs. LGU. Trudy Astronomicheskoi Observatorii Leningradskogo Gosudarstvennogo Universiteta (Reports of the Astronomical Observatory of the Leningrad State University).

Trudy GAISh. Trudy Gosudarstvennogo Astronomicheskogo Instituta im. Shternberga (Reports of the State Astronomical Institute im. Shternberg).

Trudy Stalinabad.Obs. Trudy Stalinabadskoi Observatorii (Reports of the Stalinabad Observatory).

Tsirk. Pulkov. Obs. Tsirkulyar Pulkovskoi Observatorii (Circular of the Pulkovo Observatory).

Union Circ. Circular of the Union Observatory, Johannesburg.

Usp. Astr. Nauk. Uspekhi Astronomicheskikh Nauk (Advances in the Astronomical Sciences).

V. J. S. Vierteljahresschrift der Astronomischen Gesellschaft.

Warsaw Obs. Circ. Warsaw Observatory Circular.

Warsaw Publ. Warsaw Publications.

Washington Obs. Washington Observations.

Wien Stw. Ann. Annalen der Sternwarte in Wien.

Wien Beob. Wiener Beobachtungen.

Zapiski Kiev. Zapiski Kievskogo Universiteta (Kiev University Transactions).

Zeits. f. Aph. Zeitschrift für Astrophysik.

Zeits. f. Astr. Zeitschrift für Astronomie.

1885 I (1884f). The twenty-fourth recorded apparition of the Comet Encke-Backlund. Discovered according to Backlund's ephemeris by Tempel (Arcetri) on 13 Dec. 1884; after that, observed only on 2 Jan. 1885 by Trepier (Algiers), Young (Princeton) and Barnard (Nashville). Discovered between Aquarius and Pegasus; in January and February 1885, moved east in Pisces; at the beginning of March, located in Pisces; at the end of March, descended to Aquarius, moving west; in April moved slowly through Aquarius.

Upon discovery, appeared as a faint nebulous glow (11 to 12^m). 3 Jan. 1885, Tempel reported the comet to be brighter and larger than previously, appearing as a faint nebula through a small seeker. At the beginning of January, described by observers in Strasbourg and Paris as a very faint nebula; D = 1 to 1'.5, no nucleus. 9 Jan., observers in Geneva and Strasbourg reported considerable decrease in brightness on passing near a 10^m star (9 to 10^m); measured with a 6-inch equatorial. 17 Jan., Comet Encke was larger than Comet Wolf but less condensed; Comet Wolf was more easily observed.

At the end of January and in February, brightness increased considerably. Observers in Munich reported that on 2 Feb. the comet was incomparably brighter than on 16 Jan.; nucleus definitely observed. On that day, Holetschek estimated the comet at $8^m.5$. 3, 5 and 8 Jan., Tempel (Arcetri) saw the comet through a seeker as a small nebula; rapid increase in brightness. 12 Feb. and 13 Feb., Tempel reported a faint trace of a tail. Trepier (Algiers) recorded spectroscopically the formation of the tail between 11 Feb. and 12 Feb.; 16 Feb., tail up to 15' long. Barnard (Nashville) estimated the tail at 10' on 11 Feb.; 13 Feb., 14 to 15' and 16 Feb., even longer (17 to 18'?). 21 Feb., Perigaut (Paris) with a Coudé equatorial estimated the comet as a circular 9^m nebula; at that time Holetschek gave 7^m for the intrinsic brightness. 18 Jan., Schur (Strassburg), using an 18-inch refractor, could easily see the comet on the horizon in spite of twilight and haze; bright condensation. 31 Jan., bright comet; 4, 8 and 14 Feb., very bright comet with strong condensation. 23 Feb., measured in bright twilight in spite of the bright moon (5 to 6^m?); 2 March, barely visible on the horizon (5^m?). After the perihelion passage, observed by Thome (Cordoba) with an 11-inch refractor on 27 March and 28 March and from 14 April to 22 April. In March, exceptionally faint, disappearing under the slightest illumination; in April, not fainter than 9 to 10^m.

References: A.N., 110-115; M.N., 45; V.J.S., 20: 148: Berl. Ast. Jahrb., 2, 3; A.N., 119: 63; Holetschek IV, p. 80.

Orbit: Backlund. —Mém. Acad. Petersburg 34 (8): 38; ephemeris: Berl. Ast. Jahrb. 1.

Holetschek took: 3 Jan., m = 12^m; 2 Feb., $8^m.5$; 21 Feb., 9^m; 2 March, 5^m; 27 March, 7^m; 22 April, $10^m.5$ and obtained $d_1 = 7^m.8$ to $10^m.2$. For the beginning of February 1885, $D_1 = 2'.2$ to $2'.3$; in January, $D_1 = 1'.1$ to $2'$; end of February (during twilight observations), $D_1 = 0'.8$. In C.A.M., $H_{10} = 9^m.7$. Secular variations in brilliance were studied by S.K. Vsekhsvyatskii, A.Zh., 2: 68. 1925; 31: 283. 1954; B.Yu Levin, A.Zh., 25: 246. 1948 and Link, Ann. Aph., 2. 1948. Spectrum was observed by Trepier, C.R., 100: 616. 1885; 11 Feb. to 16 Feb., S = 0.005 to 0.006.

(r, Δ): 13 Dec. 1884 —(1.60, 1.42); 4 Jan. 1885 —(1.32, 1.42); 20 Jan.—(1.08, 1.35); 3 Feb. —(0.84, 1.22); 17 Feb. —(0.59, 1.02); 3 March —(0.37, 0.73); 28 March —(0.60, 0.86); 22 April —(1.05, 1.11).

1888 II (1888b). The twenty-fifth recorded apparition of the Comet Encke-Backlund. Discovered according to Backlund's and Serafimov's ephemeris by Tebbutt (Windsor) on the evening of 8 July. Located moving south-east in Cancer; in the second half of July, passed through Sextans and Crater; in August, moved through Corvus, Hydra and Centaurus. 8 July, (10 days after the perihelion passage) Tebbutt spotted the bright circular comet with a well developed condensation 1' in diameter; coma over 6' in diameter. Rapid decrease in brightness; measurements in Australia dis-

continued on 1 Aug. 15 July and 16 July, very faint due to first-quarter Moon; 25 July, no Moon, but very faint and diffuse; no condensation; D = 2' (8 to 9^m). 31 July and 1 Aug., exceptionally faint; measured with great difficulty on an 8-inch refractor (9 to 10^m). 3 Aug. to 9 Aug., Finlay (Cape) observed the comet as a faint luminous spot with D = 2', no noticeable condensation. Under the least illumination, almost impossible to observe. The comet and the reticle, simultaneously (9 to 10^m). 28 July to 25 Aug., measured in Cordoba; very faint during the last days and hardly visible on 25 Aug. (10 to 11^m).

References: A.N., 119, 120, 122; M.N., 49; A.J., 9; V.J.S., 24; Holetschek IV, p. 82.

Orbit: Backlund and Seraphimoff.—A.N. 119: 174

Holetschek, taking m = 6^m on 8 July and m = 10^m.5 on 25 Aug., adopted H_1 = 7^m.9 and 10^m.1. In C.A.M., H_{10} = 9^m.7; 25 July D_1 = 1'.5; no tail.

(r, Δ): 8 July —(0.43, 0.98); 25 July —(0.73, 0.73); 3 Aug. —(0.89, 0.72); 25 Aug. —(1.24, 0.95);

1891 III (1891d). The twenty-sixth recorded apparition of the Comet Encke-Backlund. Spotted by Barnard (Lick Obs.) on 1 Aug. with a 36-inch refractor; D = 3/4', brightness 16^m.75 [sic]. Located in Taurus, moving east, at the beginning of September, located in Gemini; in September and the beginning of October, passed through Cancer and Leo; 12 Oct., located in Virgo.

Rapid increase in brightness; 3 Sept., Witt (Berlin) described it as very bright and large. 5 Sept., Luther (Hamburg) described the comet as a bright, large nebulous mass with a condensation but no starlike nucleus. 7 Sept., unclear though very bright nebula; D = 2'; nucleus 11^m (8 to 9^m). 12 Sept., bright with an 11^m.5 nucleus; 29 Sept., very bright with an 8^m nucleus (6 to 7^m); 30 Sept., 8^m central condensation. 4 Oct., brighter than Comet Wolf in spite of low altitude; nucleus 9^m; 5 Oct., nucleus somewhat brighter than 9^m.1. Numerous brightness estimates made by Holetschek (Vienna) with a 6 1/2-inch refractor and a 3.7-cm seeker. 9 Sept., appeared through seeker as an 8^m.1 star; 13 Sept., 8^m.0; 14 Sept., nebulous star of 6.5 to 7^m through seeker; 25 Sept., because of the Moon, only the brighter part visible (brighter than 7^m.5). 30 Sept., after emerging above the horizon, appeared through a seeker as only 0^m.5 fainter than k Leonis (6^m.3). 2 Oct., disappeared in twilight simultaneously with k Leonis (6^m). 11 Oct. and 12 Oct., remained visible more than 20 minutes after sunrise (5 to 6^m). 27 Sept. and 1 Oct., Knopf (Jena) described the comet as equal to the Andromeda Nebula (4 to 5^m).

3 Oct., Rentz (Pulkovo) observed in twilight a narrow long curving tail up to 15' long. 5 Oct., 8' tail when very low in the sky; intrinsic brightness of the coma 6 to 7^m; nucleus observed occasionally (6^m). 11 Oct., in Oxford, observed in bright twilight when no star fainter than 7^m was visible (5 to 6^m). Not observed after the perihelion passage.

References: A.N., 127-132; M.N., 52; Wien Stw. Ann., 8; Holetschek IV, p. 83.

Orbit: Backlund. —A.N., 127: 428.

Holetschek estimated H_1 from 14^m.8 (2 Aug.) to 7^m.6 (September-October). In C.A.M., H_{10} = 9^m.1; y = 8.6; H_y = 8^m.7. In Sept., D_1 = 2'.0; 3 Oct., S = 0.005. Tail apparently type I.

(r, Δ): 1 Aug. —(1.53, 1.60); 18 Aug. —(1.29, 1.28); 10 Sept. —(0.93, 0.96); 30 Sept. —(0.57, 0.96); 12 Oct. —(0.38, 1.14).

1895 I (1894d). The twenty-seventh recorded apparition of the Comet Encke-Backlund. Discovered on 31 Oct. according to Backlund's ephemeris by Perrotin (Nice) with a 76-cm refractor and by Wolf (Heidelberg) photographically; discovered independently on 1 Nov. by Cherulli (Teramo). Located in Pegasus, slowly moving south-west; at the end of December, located between θ Pegasi and α Aquarii; in January, passed through Aquarius; in February, located in Capricornus.

Upon discovery, exceptionally faint comet; in December, could be observed with medium-power telescopes. 31 Oct., $m = 13^m$; very diffuse tail; Holetschek took $12^m.5$. 18 Nov., intrinsic brightness, 12^m; 22 Nov. and 23 Nov., $11^m.7$; 2 Dec., $10^m.5$; at that time, Le Cadet gave $D = 5'$. 10 Dec., visible with difficulty in nearly full moon; 17 Dec., well visible through small seeker; estimated $8^m.7$. 22 Dec., central condensation, no starlike nucleus ($8^m.5$). 23 Dec., $m = 8^m.3$; 25 Dec., $8^m.3$ to $8^m.2$; 26 Dec., $8^m.1$; 28 Dec., $m = 8^m.0$ (from four comparison stars); 31 Dec., $7^m.0$ through seeker; 13 Jan. and 15 Jan. 1895, $m = 6^m.6$ through seeker (by comparison with stars); 17 Jan., $6^m.3$; 24 Jan., 5 to $5^m.5$ at low altitude in evening twilight; 25 Feb. (JAN.), still visible. Last position determination by Robinson (Oxford). 28 Dec., Winkler (Jena) gave $D = 3'$; 15 Jan. and 18 Jan. 1895, Schwab (Kremsmünster) gave $D = 2'$. In January, Sperra apparently saw the comet with the naked eye; at that time, a tail 1° long; 15 Jan., a tail 1 1/2° long was reported from Northsfield. Not observed after the perihelion passage.

References: A.N., 136-138; A.J., 15-17; M.N., 55; V.J.S., 30, 31; Holetschek IV, p. 86.

Orbit: Backlund. —Mém. Acad. Petersburg, 8.

Holetschek's estimates give H_1-values between $11^m.5$ and $8^m.0$. In C.A.M., $y = 10.3$, $H_y = 9^m.3$ and $H_{10} = 9^m.3$. In Dec. 1894 and Jan. 1895, $D_1 = 4'.5$ to $1'.4$; 15 Jan. 1895, $S = 0.019$.

(r, Δ): 31 Oct. —(1.75, 0.91); 23 Nov. —(1.47, 0.90); 17 Dec. —(1.12, 0.89); 31 Dec. 1894 —(0.89, 0.84); 14 Jan. 1895 —(0.64, 0.73); 25 Jan. —(0.45, 0.62).

• **1898 III (1898d).** The twenty-eighth recorded apparition of Comet Encke-Backlund. Spotted on the evening of 7 June by Grigg (Thames, New Zealand) according to his own ephemeris position only 3° above the horizon; 11 June, Tebbutt (Windsor) discovered the comet according to A. Ivanov's ephemeris. Located in Gemini, moving rapidly south; crossed Canis Minor and Monoceros, passing south of Hydra and moving in Centaurus in July.

Upon discovery, well visible in twilight through a 4 1/2-inch refractor (6^m); 25 June and 26 June, observed only through an 8-inch telescope, though still visible with great difficulty through a 4 1/2-inch refractor; appeared as a faint spot with $D = 2$ to $3'$. 27 June, invisible even through an 8-inch telescope. 10 July, having left the twilight region, the comet was visible with periphereal vision in an absolutely clear, moonless sky and as a faint white spot 5 to 6' in diameter.

References: A.N., 146, 147; M.N., 59; V.J.S., 34; Holetschek IV, p. 88.

Orbit: O. Backlund. —Mém. Acad. Petersburg, 8(2). The apparition was similar to that of 1865 II.

Taking $m = 6$, 8 and 9 to 10^m for 11 June, 26 June and 10 July, respectively, Holetschek obtained $H_1 = 8^m.5$, $10^m.8$ and $12^m.2$. In A. Zh., 4:298 and C.A.M., $H_{10} = 10^m.7$; $D_1 = 0'.9$ to $1'.5$.

(r, Δ): 7 June —(0.45, 0.72); 26 June —(0.79, 0.35); 10 July —(1.03, 0.28).

• **1901 II (1901b).** The twenty ninth recorded apparition of Comet Encke. Spotted near Thonberg's ephemeris position by Wilson (Northsfield) on the morning of 5 Aug. Located in Auriga, moved through Gemini (August), Cancer (end of August) and Leo (beginning of September) and then passed rapidly to Ophiuchus (October).

8 Aug., observers in Königsberg and Heidelberg reported a very diffuse comet lacking any sharp nucleus, $D = 1'$; 9 Aug., central condensation, nonhomogeneous nebula; 11 Aug., nucleus more obvious. 17 Aug., Abetti (Arcetri) reported bright, apparently elongated comet; 19 Aug., nebula with $D = 1'.5$, as bright as an $8^m.0$ comparison star. According to Holetschek, 18 Aug., $m = 8^m.1$; 19 Aug., $7^m.7$; 22 Aug. and 23 Aug. $7^m.5$ to $7^m.6$; 25 Aug., 8^m; 2 Sept., in bright twilight, $6^m.5$. At that time the nucleus increased in

brightness from $9^m.5$ to 8^m, D = 1'. Brightness estimates were also made in Strasbourg and Bamberg. 1 Sept., Cerulli (Teramo) reported traces of a tail at P = 250°. 4 Sept., measured last in bright twilight, at Königsberg. At the beginning of October, Tebbutt (Windsor) failed to detect the comet in evening twilight (fainter than 8 to 9^m).

References: A.N., 156-158; A.J., 21; V.J.S., 37, 38; Holetschek IV, p. 90.

Orbit: Backlund. —Mém. Acad. Petersburg, 8(2).

Holetschek, making use of his own estimates and those of other observers, obtained $H_1 = 7^m.6$ to $8^m.5$; nucleus $9^m.1$ to 10^m. In C.A.M., $H_{10} = 9^m.1$. 8 Aug. to 18 Aug., $D_1 = 1'.4$ to $1'.7$; 22 Aug. to 24 Aug., $2'.5$. S > 0.

(r, Δ): 5 Aug. —(0.98, 1.42); 15 Aug. —(0.81, 1.31); 25 Aug. —(0.63, 1.26); 4 Sept. —(0.46, 1.27).

1905 I (1904b). The thirtieth recorded apparition of Comet Encke-Backlund. Discovered according to Kamienski and Okulich's ephemeris by Kopff (Königstuhl) on 11 Sept. 1904 on a plate exposed for 3 1/2 hours. Upon discovery, very faint and diffuse; according to Wolf, $m = 12^m.0$ to $12^m.3$ (photographic); visually observed from the end of October. Located in Pisces; moved west through Andromeda (October), Pegasus (November), Delphinus and Aquila (December). Not observed after the perihelion passage.

28 Oct., Wolf, using 2-hour exposures on the Brusov telescope, photographed a faint tail extending north ($13^m.5$). 29 Oct. and 30 Oct., Holetschek failed to detect the comet with a 6-inch refractor; 8 Nov., first observation: a very faint diffuse mass, D = 3', condensation, $m \approx 11^m$; 13 Nov., $m \approx 10^m.5$; 25 Nov. nucleus 10.5 to 11^m, D≈8' (through small seeker, an exceedingly faint nebula of $9^m.0$); 26 Nov. and 27 Nov., $m \approx 8^m.6$; 28 Nov., $m = 8^m.4$ (through seeker), D = 5', nucleus 10^m. 29 Nov., $m = 8^m.3$, D = 7', condensation 10^m; 4 Dec., through seeker, large nebulous mass of $6^m.5$ to $8^m.0$, D = 7', condensation 10^m. 9 Dec., $m = 6^m.2$ (through seeker); fainter than 13 Delphini, which V. Struve in 1828 described as equal to the comet when viewed with the naked eye; considerably fainter than M 15 ($6^m.2$). 10 Dec., $m = 6^m.0$ (seeker), D = 5', condensation 9.5 to 10^m; 16 Dec., $m = 6^m.2$ (through binoculars 5.5 to 6^m), D = 5', condensation 8 to $8^m.5$, rudiments of a tail; 22 Dec., appeared brighter through seeker than 42 Aquilae ($5^m.5$). D≈5'; 23 Dec., $m = 5^m.3$, condensation ~ $6^m.3$; 27 Dec., $m = 5$ to $5^m.3$, condensation 8^m (through 3 1/2-inch refractor).

30 Oct., Hartwig (Bamberg) estimated D = 10'; 8 Dec., Nijland (Utrecht) gave $m = 7^m.6$ through binoculars; 22 Dec., $6^m.5$; 17 Dec., Abetti (Arcetri) estimated $m = 5^m.7$ through binoculars. 14 Nov., Wirtz saw a wide fan-shaped diffuse tail and a jet 3'.5 long at P = 270°; 9 Dec., $m = 6^m.5$ (seeker); 14 Dec., wide tail at P = 270°; 17 Dec., $m = 6^m.1$, D = 4'.5, tail (jet) 4'.5 long (P = 250°); 5 Dec., "fan" also reported by Barnard; 2 Dec. to 20 Dec., observed by Grachev (Kazan').

References: A.N., 166-173; A.N., 181; M.N., 65, 66; Izv. Russ. Astr. Soc., 13(8) 1908; V.J.S., 40, 41; Holetschek IV, p. 92.

Orbit: Backlund. —Mém. Acad. Petersburg, 8(?).

From all the estimates, Holetschek obtained H_1 ranging from $12^m.8$ to $7^m.9$. S. Vsekhsvyatskii, A. Zh., 4: 298. 1927, obtained y = 14.5, $H_0 = 9^m.8$, $H_{10} = 9^m.8$; same figures in C.A.M. In Oct. and Nov., $D_1 = 5'.7$ to $3'.6$; in Dec., 2'.4.

(r, Δ): 11 Sept. —(2.04, 1.21); 11 Oct. —(1.67, 0.74); 13 Nov. —(1.27, 0.51); 29 Nov. —(1.03, 0.49); 10 Dec. —(0.84, 0.48); 27 Dec. —(0.53, 0.51).

1908 I (1908b). The thirty-first recorded apparition of the short-period Comet Encke-Backlund. Not detected before the perihelion passage, in spite of the search undertaken in December 1907 and January 1908 by Wolf (Heidelberg) and in March and May 1908 by Holetschek (Vienna). The object detected by Wolf on 2 Jan. 1908 cannot be identified with Comet Encke.

Discovered according to Kamienski's ephemeris by Woodgate (Cape) on 27 May; observed photographically till 5 June when located in Eridanus and Cetus; very faint on plates. 3 June to 8 June, measured by Ross (Melbourne) on a 12-inch reflector; he estimated $m = 9^m$, $D = 3'$.

References: A.N., 177, '78; B.A.A.J., 18; V.J.S., 44; Holetschek IV, p. 96.

Orbit: Backlund. —Mém. Acad. Petersburg, 8(2).

Holetschek took $m = 8^m$ at the beginning of June and obtained $H_1 = 10^m.6$; in C.A.M., $H_{10} = 10^m.8$. 2 June to 7 June $D = 1'.0$.

(r, Δ): 27 May —(0.72, 0.39); 8 June —(0.93, 0.34).

1911 III (1911d). The thirty-second recorded apparition of the short-period Comet Encke. Discovered according to Backlund's ephemeris by Gonnessiat (Algiers) on 31 July. Visible in Gemini before sunrise, at 3° above the horizon; a white, condensed spot 30" in diameter; disappeared in the morning glow simultaneously with 10^m stars.

1 Aug., in the morning, visible on the horizon as a 9^m star; in the dark, 7 to 8^m; 2 Aug. and 3 Aug., not observed. After the perihelion passage, observed photographically at Johannesburg and the Cape; located in Leo and Virgo. 3 Sept. to 8 Sept., Wood gave $m = 9^m.5$; 9 Sept. to 24 Sept., measured by Ristenpart (Santiago) with a 24-cm refractor. 23 Sept. and 24 Sept., at the visibility threshold (10 to 11^m); at that time, $D = 1/2'$. Visible on 25 Sept. but impossible to measure.

References: A.N., 189-192; M.N., 72; V.J.S., 47, 48; Holetschek IV p. 98.

Orbit: Backlund. —A.N., 190:49. The precalculated data were quite erroneous apparently because of a misprint in recording the eccentricity.

Holetschek adopted $H_1 = 8.0$ to $10^m.4$; Vsekhsvyatskii estimated $H_{10} = 10^m.2$; Same magnitude given in C.A.M. $D_1 = 0'.7$ (in morning glow; apparently the central condensation only).

(r, Δ): 31 July —(0.59, 1.45); 1 Sept. —(0.48, 1.26); 13 Sept. —(0.70, 1.26); 25 Sept. —(0.93, 1.35).

1914 VI (1914d). The thirty-third recorded apparition of the short-period Comet Encke. Detected by Barnard (Yerkes Obs.) on 17 Sept. and independently by Neujmin (Simeis) on 20 Sept. and Thiele (Bergedorf) on 29 Sept., in all cases according to Matkiewicz's ephemeris. Upon discovery in Simeis and Bergedorf, estimated at $14^m.0$; $D = 30''$. Located in Perseus, moving north-east; in October, passed through Auriga, Lynx and Ursa Major; in November, traversed Coma Berenices and Virgo, moving to conjunction with the Sun.

14 Oct., observed by Silbernagel (Munich) as an elongated nebula without traces of condensation; negligible surface brightness; visible through a seeker; estimated at $9^m.5$. 11 Oct. to 21 Oct., photographed by Tikhov (Pulkovo) on the Bredikhin astrograph and a small camera. According to Murashkinskii, 13 Oct., $m = 9^m.9$; 21 Oct., $9^m.0$. Plates showed the motion of a protuberance in the comet's nucleus. 25 Oct., spotted by Holetschek (Vienna) as a comparatively bright nebula with a very eccentric nuclear condensation of 10^m; nebula 8 to 10' long and 5 to 6' wide; through a small seeker, the intrinsic brightness was estimated at $7^m.5$. 27 Oct., still visible; $m = 7^m$; size $10' \times 7'$. In October and November, photographed by Kostinskii (Pulkovo) on a normal astrograph. 6 Nov., Steavenson (London) observed the comet easily through binoculars; a starlike nucleus of $8^m.5$ (6 to 7^m). Plates taken by Barnard on 26 Oct. showed a slightly curved tail 2' wide; 29 Oct., $D = 18'.75$; 27 Oct., a narrow straight tail over 1° long.

22 Sept., 1916, on photographs of the presumed location of Comet Encke according to Kritzinger's ephemeris, Wolf (Königstuhl) discovered a $16^m.5$ object possessing the same motion as Comet Encke. Viljev, proceeding from the orbit corrections introduced by the Pulkovo observations, objected to the identity of the observed object with comet Encke.

References: A.N., 199-208; M.N., 75; Pop. Astr., 22, 23; Bull. Poulkovo, 8(83); Holetschek IV, p. 99.

Orbit: Matkiewicz. —A.N., 199: 427.

Holetschek from his own estimates, for 25 Oct. and 27 Oct. gave $H_1 = 9.8$ to $10^m.2$; in V.II, $H_{10} = 10^m.0$; in C.A.M., $H_{10} = 10^m.1$. The same values were given in the most recent publication, A. Zh., 31: 282. 1954. In Oct., $D_1 = 1'.6$ to $2'.9$; 27 Nov., $S = 0.012$.

Judging from the shape, the tail was of type I.

17 Oct. and 20 Oct., spectra photographed by Tikhov, A.N., 223: 279, with an objective prism. Pulkovo plates were investigated by S.K. Vsekhsvyatskii, Bull. Poulkovo, 15(6); high relative intensity of CN emission (3883 Å) and of Raffeti bands (4050 Å) in comparison with the C band 4735 Å.

(r, Δ): 17 Sept. —(1.53, 0.83); 26 Sept. —(1.42, 0.69); 12 Oct. —(1.19, 0.42); 28 Oct. —(0.93, 0.29), 23 Nov. —(0.46, 0.67).

1918 I (1917c). The thirty-fourth recorded apparition of the short-period Comet Encke. Located according to Viljev's ephemeris by Schorr (Bergedorf) on plates taken with a reflector on 30 Dec. 1917; a 15^m nucleus; D = 20". Located in Pisces, moving east; at the end of February 1918, located near η Piscium; moved through Aquarius after the perihelion passage on 24 March.

Photographed in Bergedorf. 14 Jan. 1918, two condensations observed in the coma; the fainter one 15" south-east of the main one. 16 Feb., a diffuse $11^m.5$ nucleus; $D = 0'.7$. 25 Feb., visible through a seeker (10^m). Schorr observed the comet with a 26-cm refractor. 5 March, diffuse $9^m.5$ nucleus; $D = 0'.7$. 14 March, diffuse $7^m.5$ nucleus; 15 March and 16 March, $m = 7^m.5$; low in the sky, observed through tree branches. 1 March and 2 March, van Biesbroeck (Yerkes Obs.) saw a circular nebula $D = 0'.9$ (central condensation ?); $m = 7^m.8$ through a 3-inch seeker. In March, observed in Greenwich. 1 March, $D = 2'$. 9 March, more condensed; $m = 8^m.3$. 12 March, $m = 7^m.7$; $D = 1'.5$. In January, observed in Tacubaya.

After the perihelion passage, observed in Melbourne from 17 April to 21 April; 17 April, no definite nucleus; 20 April, faint and diffuse.

References: A.N., 204-207; A.J., 32; M.N., 78; Pulkovo Bull., 14: 123.

Orbit: Viljev. —A.N., 205: 124.

In C.A.M., $H_{10} = 10^m.6$. When r = 0.6, $H_{10} = 9^m.9$ according to Vsekhsvyatskii. — A. Zh., 31: 286. In March, $D_1 = 2'.5$.

(r, Δ): 30 Dec. 1917 —(1.60, 1.67); 14 Jan. 1918 —(1.41, 1.66); 3 Feb. —(1.11, 1.56); 19 Feb. —(0.85, 1.39); 7 March —(0.56, 1.12); 15 March —(0.42, 0.93); 16 April —(0.66, 0.74); 28 April —(0.87, 0.84).

1921 IV (1921d). The thirty-fifth observed apparition of the short-period Comet Encke. Detected by Skjellerup and Reid (Cape Observatory) on 27 July (8 to $9^m.5$) as an 8 to $9^m.5$ object in Sextans near the horizon. Moved south-east; 13 Aug., located in Corvus.

Observed only in Capetown, Johannesburg and also in Santiago with a 9-inch refractor. 7 Aug., no nucleus, faint object inconvenient for measuring; much fainter and diffuse than Comet Pons-Winnecke on the same night (9.5 to 10^m). 8 Aug., very faint; difficult to measure (10 to $10^m.5$). 13 Aug., very faint (10.5 to $11^m.5$). 22 Aug. and 23 Aug., not spotted in a dark sky (fainter than $12^m.0$). 30 July, reported in Santiago as a diffuse nebula with a bright condensation. 9 Aug. and 10 Aug., difficult to observe through a 28-cm refractor.

References: A.N., 214, 218; B.Z., 3; Pulkovo Bull., 14: 123.

Orbit: Matkiewicz. —M.N., 82: 269.

In E-I, $H_{10} = 10^m.8$; proceeding from these estimates, $H_{10} = 11^m.2$ to $11^m.5$.

(r, Δ): 27 July —(0.50, 0.99); 6 Aug. —(0.67, 0.90); 14 Aug. —(0.82, 0.88).

Assumed second apparition of the short-period Comet Neujmin (2). Neujmin showed that the 15 to 16^m object observed on 16 June 1921 on double-astrograph plates was not Comet Neujmin (2). Circ. Pulkovo Obs., 32: 27.

1924 III (1924b). The thirty-sixth recorded apparition of the short-period Comet Encke-Backlund. Discovered according to Matkiewicz's ephemeris by van Biesbroeck (Yerkes Obs.) on 31 July; estimated at 16^m. Registered at the same time by Merton (Greenwich) on a 30-inch reflector plate as a 15^m object. Later, the comet was also discovered on a plate taken on 28 July; $m = 17^m$. Located near Pleiades, moving north-east through Perseus (August), Auriga (September), Leo and Virgo (October), as it approached conjunction with the Sun.

Upon discovery, van Biesbroeck reported an elongation at P = 60°. 24 Aug., faint diffuse nebula with a hardly noticeable condensation, D = 0'.3, $m = 15^m$; 28 Aug., D = 1'.3, $m = 14^m.5$. 3 Sept., visible through a 4-inch seeker as a faint nebula with a 15^m nucleus and a short 1'.5 tail at P = 80°; 16 Sept. easily visible through a 4-inch seeker, $m = 11^m$, diffuse nucleus. 21 Sept., $m = 9^m.0$ through a seeker, in spite of moonlight; head extending east over 2' from the nucleus. 23 Sept., $m = 8^m.8$ (seeker), nucleus 12^m. 5 Oct., photographs taken with a 24-inch reflector showed, apart from the wide tail, a faint, narrow, slightly serpentine tail at P = 305° (8' from the nucleus). 7 Oct., $m = 8^m$?; coma extending east over 2' from the nucleus. 13 Oct., $m = 7^m.0$; 17 Oct., $7^m.0$; 20 Oct., $6^m.8$, yet hardly visible when low in the sky.

5 Sept., observed by Dubyago (Kazan'): $m = 12^m.5$, D = 2'. 23 Sept. to 5 Oct., Vorontsov-Vel'yaminov and Vsekhsvyatskii (Kuchino) described the comet as a circular nebula, D = 2', varying in brightness from $9^m.0$ to $8^m.1$. 26 Sept., Plakidis (Athens) estimated $8^m.5$ through a seeker. 4 Oct., $8^m.0$; eccentric condensation with a $12^m.5$ to $13^m.0$ nucleus. 7 Oct., $7^m.5$; 9 Oct., $7^m.0$, D = 1'.5.

3 Sept., Bower (Washington) reported $m = 13^m$; comet diffuse in appearance under poor visibility conditions. 14 Oct., $8^m.0$. 21 Oct., a 20' tail in twilight; P = 303°. Photographed by Kostinskii (Pulkovo) on a normal astrograph and by Jeffers (Lick Obs.), who gave D = 2' on 28 Sept. Observed also at Bergedorf, Pulkovo, Moscow, Vienna, Algiers, Sonneberg and Copenhagen. Measured last at the Yerkes Observatory on 24 Oct. in a bright sky.

References: B.Z., **6**; A.N., **222-226**; A.J., **36**; J.Obs., **7**; M.N., **85**; V.J.S., **60**.

Orbit: Matkiewicz. —Izv. Pulkovo Obs., **14**: 123.

From his own estimates, van Biesbroeck obtained y = 15, $H_{10} = 11^m.5$. Vsekhsvyatskii, A.Zh., **4**: 300, using the photometric estimates of Vorontsov-Vel'yaminov and his own estimates obtained $H_{10} = 9.6$ to $10^m.3$; In C.A.M., $H_{10} = 10^m.0$. In his last reappraisal Vsekhsvyatskii, A.Zh., **31**: 287, obtained on the average $H_{10} = 10^m.68$. In Sept. and Oct., $D_1 = 2'.3$. 21 Oct., S = 0.006.

Spectrum photographed by Tikhov, A.N., **223**: 27, with a 13° prism on the Bredikhin astrograph. These spectrograms were investigated photometrically by Vsekhsvyatskii, Izv. Pulkovo Obs., **15**(6).

(r, Δ): 31 July —(1.71, 1.71); 17 Aug. —(1.49, 1.35); 2 Sept. —(1.27, 1.05), 18 Sept. —(1.02, 0.82); 4 Oct. —(0.74, 0.76); 24 Oct. —(0.41, 1.03).

1928 II (1927h). The thirty-seventh recorded apparition of the short-period Comet Encke-Backlund. Discovered according to Matkiewicz's ephemeris by van Biesbroeck (Yerkes Obs.) on 13 Nov. 1927 as a circular nebula, D = 24", $m = 16^m$, distinct nucleus.

After discovery, spotted on plates of 19 Oct. and 20 Oct. as a 17^m object. Located in the south-east part of Pegasus, slowly retrogressed; in January, passed through Pisces; in February, rapidly descended south, moving through Aquarius and Capricornus.

Before the perihelion passage, spotted and observed on 17 Jan. 1928 by Tikhov (Pulkovo) on the Bredikhin astrograph and by Pokrovskii on the 15-inch refractor. 20 Jan. and 23 Jan., photographed by Deich on the normal astrograph; estimated at $9^m.5$ with an $11^m.0$ nucleus. 23 Jan., Tikhov obtained a high-quality spectrogram with an objective prism mounted on the Bredikhin astrograph; the spectrogram showed all the characteristic cometary

bands. 4 Feb. and 5 Feb., Martynov and Dubyago (Kazan') reported a 4 to 8' tail and a clear nucleus. At that time, van Biesbroeck's photographs showed a clear nucleus and a wide 5' tail pointing west; $m = 8^m$. In January and February, Steavenson reported $m = 6^m$; nearly circular $D = 2'$, an almost starlike nucleus situated eccentrically on the eastern side of the coma. Last observation before conjunction with the Sun was by van Biesbroeck on 12 Feb. when the comet was a nebulous 8^m object low in the sky soon after sunset. After the conjunction, observed photographically in Johannesburg from 20 March to 3 April as an 11 to 12^m object.

References: B.Z., 9; A.N., 231-233, 236; M.N., 88; Obs., 51; Pop. Astr., 35, 36; A.J., 38; V.J.S., 64-66; Izv. Pulkovo Obs., 14: 6.

Orbit: Matkiewicz. —A.N., 231: 11.

In E-I, according to the February estimates of van Biesbroeck, $H_{10} = 11^m.0$; making use of all the available estimates, A. Zh., 31: 281, $H_{10\,(av)} = 11^m.8$, at $r = 0.6$, $H_{10} = 10^m.0$. According to Link, $H_{10} = 12^m$. In Feb., $D_1 = 1'.6$, in March, $0'.4$. $S = 0.002$. Tail types were not studied.

Spectrum studied by Vsekhsvyatskii, Izv. Pulkovo Obs., 15(129): 6.

(r, Δ): 19 Oct. —(2.06, 1.11); 13 Nov. —(1.78, 1.09); 10 Dec. 1927 —(1.44, 1.13), 19 Jan. 1928 —(0.82, 0.99); 4 Feb. —(0.52, 0.80); 20 March —(0.82, 1.24); 7 April —(1.09, 1.40).

1931 II (1931a). The thirty-eighth recorded apparition of the short-period Comet Encke-Backlund. Detected according to Matkiewicz' ephemeris by Bobone (Cordoba) the evening of 21 June as a $9^m.0$ nebula in Canis Minor. Later, it was learned that the comet had been discovered and measured on plates taken by Wood (Johannesburg) on 14 June and 16 June to 21 June; observed at Johannesburg till 17 Nov. Moved rapidly southeast, receding from perihelion; passed through Hydra and Centaurus.

14 June, $m \approx 7^m$; 5 July and 6 July, faint; 14 July, good image; 17 July, very faint; 5 July and 17 July, observed by Thomson (New Zealand), who estimated $m = 8$ to $9^m.4$; on a 15 July plate Bobone estimated $m = 12^m$. In January 1932 van Biesbroeck failed to spot the comet.

References: B.Z., 13; A.N., 243; Obs., 54; B.S.A.F., 46; A.J., 41, 42; Izv. Pulkovo Obs., 14 (123).

Orbit: Matkiewicz. —A.N., 242: 141.

In C.A.M., $H_{10} = 11^m.0$; A. Zh., 31: 282, $H_{10} = 11^m.5$ to $11^m.3$.

(r, Δ): 14 June —(0.43, 0.77); 30 June —(0.72, 0.43); 18 July —(1.03, 0.34).

1934 III (1934a). The thirty-ninth recorded apparition of the short-period Comet Encke. Located according to Matkiewicz's ephemeris by Jeffers (Lick Obs.) on a plate taken on 10 July with the Crossley reflector; a 15^m object near the Pleiades.

After discovery, van Biesbroeck (Yerkes Obs.) detected the comet on a plate of 8 July. Moved east through Taurus, Auriga (July, August), Gemini, Cancer (August), Leo (September), Virgo (September, October) and Libra (October). Van Biesbroeck reported $m = 15^m.5$; a circular coma with $D = 15''$ and very weak condensation. 15 July, $m = 15^m$, very diffuse coma, $D > 24''$; 18 July, $m = 14^m.5$, $D = 18''$ no nucleus; 17 Aug., $m = 9^m.5$, nucleus $10^m.5$, wide tail over 3' long at $P = 30°$; 18 Aug. to 21 Aug., $m = 8.5$ to $9^m.0$, nucleus 9 to 10^m, $D = 18''$, tail at $P = 75°$; 30 Aug., at dawn, $m = 6^m.3$ through a comet seeker.

21 Aug., Jeffers gave $m = 13^m$, $D = 42''$. 9 Aug., Kotsakis (Athens) described the comet as very diffuse and irregular, $m = 13^m$; 12 Aug., $m = 11^m$, elongated, visible through an 8-cm seeker; 14 Aug., well visible through a seeker (10^m); 20 Aug., $m = 9^m.5$; 29 Aug., Adamopulos (Athens) gave $m = 9^m.0$. Also observed at Engelhardt Observatory, Kazan', Madrid and other places.

References: B.Z., 16; A.N., 252-254; Obs., 57; Pop. Astr., 42, 45; A.J., 45.

Orbit: Matkiewicz. —Circ. Pulkovo Obs., 10.

In E-I, $H_{10} = 11^m.2$; after reappraisal, Vsekhsvyatskii, A. Zh., 31: 287. 1954, gave $H_{10} = 11^m.6$. In July, $D_1 = 0^m.8$; $S > 0.0012$.

(r, Δ): 8 July —(1.41, 1.88); 25 July —(1.16, 1.59); 12 Aug. —(0.74, 1.34); 30 Aug. —(0.50, 1.27).

1937 VI (1937h). The fortieth recorded apparition of the short-period Comet Encke-Backlund. Spotted according to Crommelin and Matciewicz's ephemeris by Jeffers (Lick Obs.) on 3 Sept. as a diffuse 18^m object in Triangulum. Moving north-west, passed through Andromeda (September, October), Lacerta (November), Cygnus, Vulpecula and Aquila (November); in December, located in Ophiuchus.

Jeffer's photographs in September and October showed a sharp nucleus with a faint coma that on 9 Oct. extended into a 48" fan-shaped tail pointing north-west. According to van Biesbroeck (Yerkes Obs.), 7 Oct., $m = 15^m$, D = 18", very well-developed condensation; 27 Oct., $13^m.8$ starlike nucleus of 14^m, coma elongated by 1' at P = 310°. 3 Nov., 12^m; visible through 4-inch seeker; a fan-shaped coma diverging at 70 to 280°; eccentric nucleus. 4 Nov., 11^m; nucleus appeared to be detached from the coma. 10 Nov., 10^m; a 13^m nucleus at the apex of the coma; tail axis at P = 265°. 24 Nov., $7^m.6$ 29 Nov., $7^m.6$, diffuse coma tail at P = 260°; 30 Nov., $6^m.0$.

Photographs taken by Quenisset (Juvisy) on 25 Nov. and 29 Nov. showed a fan of jets towards the Sun and a coma elongated away from the Sun. Beyer (Hamburg) 27 Oct. to 28 Nov. reported the brightness varying from $9^m.5$ to $6^m.0$; D≈5 to 6'. According to Fedtke (Königsberg), 5 Dec., $m = 6^m.2$; according to Loreta (Bologna) and Rigollet (Nemours), 28 Nov., $m = 5^m.5$. On photographs taken by Stobbe on 27 Nov. and 28 Nov., $m_{phot} = 5^m.4$, D = 25'. The comet was sometimes visible to the naked eye at the beginning of December; envelopes were observed on the sunward side. 6 Dec., Quenisset described the comet as very bright when low over the horizon; $m = 5^m$.

Observed also at Warsaw, Nice, Tashkent, Turino, Pino Torinese, Birmingham, and other places.

References: B.Z., 19, 20; A.N., 265; Obs., 60, 61; M.N., 98; Pop. Astr., 45, 46; A.J., 47; B.S.A.F., 51, 52; B.A.A.J., 48.

Orbit: Crommelin. — B.A.A. Hbk., 1937.

Beyer, A.N., 265: 46, gave y = 14.9, $H_y = 10^m.0$; in E-IV, $H_0 = 12^m.3$, y = 20, $H_y = 12^m.0$ (very doubtful). In the most recent publication Vsekhsvyatskii, A. Zh., 31: 286, determined the mean parameter of the comet for the epoch 1935: y = 14.6, $H_y = 11^m.5$; for the 1937 apparition, $H_{10} = 10^m.4$. The mean brightness curve is represented sufficiently well by the following formulas: $H_\lambda = 11^m.35 + 13^m.7\,(\sqrt{r} - 1)$ and $H_\Delta = 11^m.0 + 6^m.5\,(r - 1)$. $D_1 = 1'.7$ (visually in Oct. and Nov.), $D_1 = 8'$ (photographically in Nov.). S = 0.0006.

Spectrum photographed by Dufay, Ann. Aph., 11: 107, and studied by Swings, Ann. Aph., 11: 128.

(r, Δ): 3 Sept. —(1.98, 1.29); 20 Sept. —(1.78, 0.95); 7 Oct. —(1.58, 0.62); 24 Nov. —(0.85, 0.30); 10 Dec. —(0.56, 0.45).

1941 V (1941b). The forty-first recorded apparition of the short-period Comet Encke. Photographic discovery by van Biesbroeck (Yerkes Obs.) on 19 Jan.; a tiny 17^m nebula in Pisces near Matkiewicz and Crommelin's ephemeris position. Located near the horizon, remaining a faint diffuse object in Pisces till March.

25 Jan., van Biesbroeck estimated $m = 16^m.5$, D = 21"; 16 Feb., 15^m, D = 24"; 19 Feb. and 20 Feb., $14^m.5$ to 14^m, D = 36" to 42"; 1 March, 13^m. Coma appeared elongated to the Sun; activization apparently began when r = 1. In summer should have been brighter and visible in the southern hemisphere, but the comet was not observed after having emerged from the solar rays.

References: Pop. Astr., 49; H.A.C., 561; I.A.U.C., 844; A.J., 50; B.Z., 22, 23.

Orbit: Makower. —M.N., 112(3).

E-IV obtained, from van Biesbroeck's estimates, y = 19, H_y = 11^m.2, H_{10} = 12^m.4; same values obtained by Vsekhsvyatskii. In Feb., D_1=1'.1 to 1'.9.

(r, Δ): 19 Jan. —(1.66, 2.01); 17 Feb. —(1.26, 1.90); 5 March —(1.01, 1.74).

1947 XI (1947i). The forty-second recorded apparition of the short-period Comet Encke. Discovered very close to Matkiewicz' ephemeris by Jeffers (Lick Obs.) on 14 Aug. as an 18^m object with central condensation D=2'. Located near Pleiades; moved north-east through Perseus (September), Auriga (September, October), Lynx (October), Leo Minor, Leo (October) and Virgo.

21 Sept., Jeffers reported m = 14^m, starlike nucleus of 16^m and a fan-shaped tail 42" long pointing north-east. In the middle of October, van Biesbroeck (Yerkes Obs.) estimated m=11^m; fan-shaped coma 4' in diameter; a clear nucleus; comet elongated 7' sunward. 12 Oct., Martynov (Engelhardt Obs.) reported m = 9^m. 10 Oct. to 12 Oct., Mazur and Pogozhevski (Cracow) gave m = 9.0 to 8^m.7; 14 Oct. and 15 Oct., 8^m.5; 20 Oct., 7^m.8; 25 Oct., 6^m.8; 4 Nov., 7^m.3; 8 Nov., 6^m.8. 25 Oct., Rijves (Tartu) reported m=9.3 to 9^m.7. 17 Oct., Giclas (Lowell Obs.) gave m = 9^m.1; 4 Nov., 7^m; 8 Nov., 5^m.3; 15 Nov., 5^m. Beyer (Bergedorf) observed the comet from 12 Sept. to 30 Oct. Last observation before disappearance in the solar rays was at Tokyo; m = 5^m.5.

References: H.A.C., 835 ff.; I.A.U.C., 1103-1115; Astr. Tsirk., 88 ff.; P.A.S.P., 59; M.N., 108; A.J., 54, 55; Obs., 67.

Orbit: Makower. —M.N., 112(3).

Vodop'yanova, from 40 estimates, obtained y = 14.8, H_y = 10^m.9, H_{10} = = 10^m.6, Beyer, A.N., 279: 51, from his own estimates, obtained y = 16, H_y = 9^m.9. In Aug., D_1 = 3', in Oct., 1'.7. S = 0.0008 (anomalous sunward tail or jet). Slit spectrograms obtained at the McDonald Observatory were investigated by Swings, Ann. Aph., 11: 124.

(r, Δ): 14 Aug. —(1.84, 1.56); 14 Sept. —(1.46, 0.91); 10 Oct. —(1.08, 0.48); 25 Oct. —(0.83, 0.43); 8 Nov. —(0.57, 0.61); 23 Nov. —(0.35, 0.99).

1951 III (1950e). The forty-third recorded apparition of the short-period Comet Encke. Detected on a plate of 21 July 1950 by Cunningham (Mt. Wilson) as a starlike object of 21^m; 16 Aug. and 17 Aug., 20^m. Moved through Pisces (June to September); then retrogressed through Pegasus (October, November) and Pisces (January to March 1951).

In December 1950, a starlike nucleus of 18^m and a faint coma of D = 1'. 7 Jan. and 8 Jan. 1951, photographed by Rozhkovskii (Alma-Ata); m = 16^m; D = 3'.5; western edge relatively brighter. 26 Jan., Martynov (Engelhardt Obs.) gave m = 14^m.5; 1 Feb., 13^m.5; 6 Feb. and 7 Feb., 13^m, faint nucleus and a coma on the sunward side; 14 Feb., 11^m (?). 11 Feb., Bakharev (Stalinabad), using 7-cm binoculars estimated m = 11^m at low altitude (8 to 10°) and on bright background; D = 2'. 19 Feb., 9^m, central condensation; 25 Feb., 8^m.3; 2 March, 7^m.4. 4 March, observations in Alma-Ata gave m = 8^m.7; D = 7'.

According to van Biesbroeck, 1 Nov. to 5 Nov. 1950, m = 17^m.5, very diffuse coma with D = 30"; 13 Nov., 14 to 17^m; 11 Dec., 16^m.5; 6 Jan. 1951, 14^m, nucleus, fan-shaped coma over 1' at P = 300°; 8 Jan., 13^m.5, wide fan-shaped tail up to 2' long at P = 260°, nucleus; 2 Feb., 11^m, tail at P = 290°; 5 Feb. to 8 Feb., 10^m, tail over 24" from the nucleus at P = 270°; 28 Feb., 8^m.1, almost circular coma with D = 1'.5, nucleus; 5 March, 7^m.1; 10 March, ~10^m in moonlight.

According to Beyer (Bergedorf), 25 Jan., m = 11^m.0, nucleus 13^m, D = 3'.5; 30 Jan., m = 10^m.6; 7 Feb., 10^m.2, D = 4'.1; 21 Feb. and 22 Feb., 8^m.7, nucleus 10^m, D = 6' to 5'; 24 Feb. and 25 Feb., 8^m.2, nucleus 10^m.5, D = 6' to 5'; 27 Feb. and 28 Feb., 7^m.9 and 7^m.8, D = 6'.6, tail 15' at P = 50°; 3 March, 7^m.4, D = 6', tail 10'; 4 March and 5 March, 7^m.3 to 7^m.2, nucleus 9^m.0, D = 6', tail 15'; 6 March, 7^m.3, nucleus 8^m.8, D = 5', tail 12'.

19 April, Johnson (Johannesburg) observed the comet as a diffuse object with a faint 10^m.0 nucleus; grew rapidly faint by the beginning of May. Observed last by Jeffers (Lick Obs.) on 7 Aug. 1951; m = 18^m.

References: I.A.U.C., 1287; H.A.C., 1115 ff.; Astr. Tsirk., **105-116**; M.N., **112**; P.A.S.P., **63, 64**; Pop. Astr., **58, 59**; A.J., **58**.

Orbit: Makower —M.N., **112**(3).

According to Vsekhsvyatskii, A. Zh., **31**: 287, H_{10} = 12^m.3; according to Vodop'yanova (36 estimates), y = 13.7, H_y = 11^m.9, H_{10} = 11^m.9; noticeably fainter after perihelion; Beyer's 14 observations, A.N., **282**: 153, gave y = 6.8, H_y = 9.8, h_0 = 11^m.8, D = 5'; S = 0.004.

(r, Δ): 21 July —(3.01, 2.70); 19 Aug. —(2.81, 2.10); 20 Sept. —(2.56, 1.59); 23 Nov. 1950 —(1.95, 1.43); 2 Jan. 1951 —(1.46, 1.52); 3 Feb. —(0.98, 1.38); 27 Feb. —(0.55, 1.04); 15 March —(0.34, 0.69); 4 April —(0.59, 0.81); 4 May —(1.11, 1.06); 7 Aug. —(2.27, 1.27).

1954 IX (1953f). The forty-fourth recorded apparition (52nd return) of the short-period Comet Encke. Discovered 10 months before the perihelion passage by Cunningham on plates taken with a 100-inch reflector. Observed on 3, 4, and 5 Sept. 1953 near ψ Piscium, as a 19^m.9 object. 4 Feb. and 5 Feb. 1954, observed by van Biesbroeck as a small 19^m nebula. 22 July and 27 July, Jones described the comet as a diffuse 19^m.7 object. Last position given by Brouwer (Johannesburg) on 27 July.

References: I.A.U.C., 1423; Astr. Tsirk., **135, 143**; Obs., **74**; B.A.A.J., **64**.

Orbit: Makower. —Astr. Tsirk., **135** and M.N., **114**: 364.

Absolute magnitude from Vodop'yanova (6 estimates).

r: 3.4, 2.3.